Journal of
Marine Science and Engineering

IMPACT FACTOR 2.7

CITESCORE 4.4

Article

Finite Element Modelling on the Mechanical Behaviour of Marine Bonded Composite Hose (MBCH) under Burst and Collapse

Chiemela Victor Amaechi, Cole Chesterton, Harrison Obed Butler, Zewen Gu, Agbomerie Charles Odijie, Facheng Wang, Xiaonan Hou and Jianqiao Ye

Special Issue
Marine Application of Fiber Reinforced Composites

Edited by
Dr. Felice Rubino, Dr. Luca Boccarusso and Dr. Fausto Tucci

MDPI

https://doi.org/10.3390/jmse10020151

Journal of *Marine Science and Engineering*

MDPI

Article

Finite Element Modelling on the Mechanical Behaviour of Marine Bonded Composite Hose (MBCH) under Burst and Collapse

Chiemela Victor Amaechi [1,2,*], Cole Chesterton [3], Harrison Obed Butler [4], Zewen Gu [1], Agbomerie Charles Odijie [5], Facheng Wang [6], Xiaonan Hou [1] and Jianqiao Ye [1,*]

1 Department of Engineering, Lancaster University, Lancaster LA1 4YR, UK; z.gu4@lancaster.ac.uk (Z.G.); x.hou2@lancaster.ac.uk (X.H.)
2 Standardisation Directorate, Standards Organisation of Nigeria (SON), 52 Lome Crescent, Wuse Zone 7, Abuja 900287, Nigeria
3 Power Plant Development Department, EDF Energy, Bridgewater House, Counterslip, Bristol BS1 6BX, UK; cole.chesterton@sky.com
4 DTU Energy, Danmarks Tekniske Universitet, 2800 KGS Lyngby, Denmark; S192084@student.dtu.dk
5 Department of Engineering, MSCM Limited, Coronation Rd., High Wycombe HP12 3TA, UK; charlesodijie@hotmail.com
6 Department of Civil Engineering, Tsinghua University, Beijing 100084, China; wangfacheng@tsinghua.edu.cn
* Correspondence: c.amaechi@lancaster.ac.uk (C.V.A.); j.ye2@lancaster.ac.uk (J.Y.)

Abstract: Currently, the properties of composites have been harnessed on pipelines in the marine offshore industry. In this study, marine bonded composite hose (MBCH) is presented. It is aimed at understanding the stress/strain distribution on marine bonded hoses using local design pressure under burst and collapse cases. This study also investigates composite material modelling, hose modelling, liner wrinkling, helical spring deformation, and two MBCH models—with and without ovalisation. The ovalized model is considered the simplified model in this research. A mesh study was carried out on meshing the hose layers. In this study, local design pressure was considered and not operational pressure. This finite element model was adopted to predict the deformation and mechanical response behaviour of MBCH. From this study, composites could be considered to improve conventional marine hoses. The study findings include identification of buckled sections on the hose and stressed zones on the helix reinforcement. Highly reinforced hose ends are recommended in ends of the MBCH as they had maximum stress and strain values.

Keywords: marine bonded composite hose; finite element model; composite riser; layered marine structures; helix spring; liner wrinkling; numerical model; stress analysis; bonded model

check for updates

Citation: Amaechi, C.V.; Chesterton, C.; Butler, H.O.; Gu, Z.; Odijie, A.C.; Wang, F.; Hou, X.; Ye, J. Finite Element Modelling on the Mechanical Behaviour of Marine Bonded Composite Hose (MBCH) under Burst and Collapse. *J. Mar. Sci. Eng.* **2022**, *10*, 151. https://doi.org/10.3390/jmse10020151

Academic Editors: Felice Rubino, Luca Boccarusso and Fausto Tucci

Received: 24 November 2021
Accepted: 17 January 2022
Published: 24 January 2022

Publisher's Note: MDPI stays neutral with regard to jurisdictional claims in published maps and institutional affiliations.

1. Introduction

The oil and gas industry has implemented a variety of technologies and hardware options to extract raw fossil fuels [1–6]. These petrochemical raw materials include crude oil and natural gas. These raw materials are refined into useable products produced using conduit hoses and marine risers [7–11]. Typical methods for the mass exploitation of natural fossil fuel reserves include permanent setups, mobile setups of dry platforms, and moored offloading/loading systems [12–15]. These installations have a complex network of marine risers and hoses connected to the platforms. [16–19]. Conversely, other components are installed directly upon oil reserve wells to extract oil. Hence, there are many techniques for deploying marine hoses and marine risers, from shallow to deep water environments. These techniques involve multiple options of hose-riser configurations, structural hose-riser designs, material selection, hose-riser manufacture, buoy design, corrosion resistance, and hose deployment [20,21]. Figure 1 shows an image of marine hoses on a rack. Typical ocean engineering applications include deployment of marine hoses on reel-mounted

FPSO (floating production, storage, and offloading) vessel/unit for (a) reel-laying and (b) ship-to-ship catenary connections.

Figure 1. Image of marine hoses on a rack. (Courtesy: Trelleborg; adapted with permission.).

Generally, floating offshore structures (FOS) support conduits like marine hoses. In recent years, the oil and gas industry has been harnessing composites and elastomeric material properties to manufacture marine hoses. These multi-layered marine tubular structures experience different structural issues such as buckling, liner failure, delamination, and matrix cracking of the layers of the structures. Similar mechanical behaviour has been reported on composite tubes and hoses [22–27]. This study presents a solution called marine bonded composite hose (MBCH) to solve a current problem facing the oil and gas industry on reeling hoses. Previous investigations have been conducted on the dynamic response of the marine hoses when attached to the Catenary Anchor Leg Mooring (CALM) buoy [28–31]. However, recent developments portray various hose patents by the hose manufacturers such as Dunlop Continental Oil & Gas, Yokohama, Trelleborg, etc. [32–36]. Currently, the industry has accepted, to some degree, the implementation of different composite materials in the design and manufacture of marine risers called composite risers [37–40]. These developments exist in recent academic reports and current industrial products from Airborne Oil & Gas, Magma Global, Technip, etc. [41–44], such as Magma's M-Pipe [45]. However, there is a challenge in applying new dynamic methods for deploying these risers while maintaining a high service life in deep water environments, such as further increasing fossil fuel extraction from harder-to-reach reserves. Secondly, these multi-layered risers have similar behaviour to marine hoses in mechanical performance. They both exhibit some mechanical-related behaviours in terms of delamination, contacts, liner collapse, and fatigue [46–51]. In principle, these marine hoses are designed using both global and local designs [52–55]. The global design considerations for marine hoses includes the motion behaviour and environmental conditions [56–61]. On the other hand, the local design considerations for marine hoses include the forces, the pressure loads, and deployment operations. These operations include installation, reeling, transfer, pipe-laying, and fluid

transportation [62–66]. While improving the service life in deep water environments, this research will improve the use of marine reeling hoses. This can assist with increasing fossil fuel extraction from harder-to-reach reserves using these unique technologies. Another recent problem that has been encountered in the implementation of deploying marine composite hose-riser systems for fluid transfer via the use of a reeling drum mounted upon an FPSO is the crushing load on the hoses. Recent examples of the use of marine hoses have reported unexpected structural hose failure [67,68], and structural mooring failure of the CALM buoy-hose system [69–71]. These failures are significantly quicker than estimated in the hose's design phase and cost the industry millions in replacement for these hoses, thus risking the viability of these risers as a sustainable method of fossil fuel extraction. Analytical and numerical investigations on composite tubular structures are also considered. Xia et al. [72] presented an analysis of multi-layered filament–wound composite pipes under internal pressure. They presented analytical formulations on the composite elastic theory using a cylindrical pipe section, which considered three-dimensional (3D) elastic constants that have effective properties for thick laminates developed in an earlier study by Sun and Li [73]. Ye and Soldatos [74] investigated 3D buckling analysis of laminated composite hollow cylinders and cylindrical panels and presented profiles of the buckling modes. Bakaiyan et al. [75] examined multi-layered filament–wound composite pipes under combined internal pressure and thermomechanical loading with thermal variations. Based on the mechanical behaviour of marine hoses, Gao et al. [76] investigated the structural behaviour of ring-stiffened composite marine rubberised hose under internal pressure and validated the model. Nassiraei and Rezadoost [77,78] numerically investigated the effect of the composite material in marine structures using ANSYS, by considering the static capacity and local joint flexibility (LJF) of tubular joints having fibre-reinforced polymer (FRP) reinforcements under different loads. Gonzalez et al. [79] investigated the axial characteristics of flexible bonded marine hoses and presented some hose bending profiles. In the same vein, different researchers also presented mathematical models with numerical solutions on marine hoses' static and dynamics analysis [16,57–59,80]. Lassen et al. [81] presented an investigation on the load response of a marine bonded hose and its helix reinforcement, while Tonatto et al. [82] investigated the composite rings and spirals of an offshore hose. From these aforementioned investigations, the internal pressure loads were recorded as the most critical loads since they presented the highest stresses on the layers of the structures investigated. Another challenge is the material modelling of the composite tube or helical spring reinforcement. Thus, there is an imminent need for a better understanding of the industry's problem today, at both local and global levels, to further advance the use of composite materials in hose-riser applications.

This research presents the studies conducted on the local design of marine bonded hoses under internal pressure and external pressure using the finite element modelling (FEM). Based on the local analysis, the aim was to model a reeled section of the tubular marine riser structure. Bonded contacts were utilised for the multi-layers. From the modelling in Sections 2 and 3, it was possible to simulate the stresses experienced on this section of the hose-riser to identify potential failure modes of the structure under the state as described in actual cases of hose/riser failure. The analysis of the stresses on these hose sections can be used to develop the global design model in further studies, for structural verification and postprocessing. The boundary conditions for the FEM were conducted in Section 3, while Section 4 shows FEM results of the novel MBCH structure and presents discussions on the results. The concluding remarks are provided in Section 5.

2. Materials and Methods

2.1. Model Description

For the local design of the reeling hose, ANSYS Structural version R2 2020 [83,84] and Simscale OpenFEA [47,85] were utilised. Both platforms were used to ascertain the different physics investigated on the loading conditions of the marine reeling hose to present results from both statics and dynamic behaviour of the hose. The sections of the

reeled and the unreeled hose are shown in Figure 2. The geometric parameters and the material properties of the hose are presented in Sections 2.3 and 2.4. In the present study, the ANSYS benchmark is used rather than ANSYS APDL due to the need for modelling demand to use a different package in modelling this marine hose. It is noteworthy that this is a highly multi-layered marine structure, with various contacts and layers. As such, under higher licenses, the ANSYS platform was limited to its performance in running the ANSYS model under higher element numbers while producing the results in faster time. Thirdly, there was another limitation of running the Finite Element Analysis (FEA) in high-performance computers (HPC) for this model. Hence, an Open-Source Aster Code embedded within Simscale Open FEA was considered, as it is faster, reliable, verified, and could produce more case studies for our model. Lastly, in this model, symmetry was considered but applied not in the present study but in another study that is not included in this present paper. In the present study, symmetry was not very representative due to the spiral arrangement of the spring. However, it would have reduced computational cost, as we found in the second model used in a separate study but not in the present study.

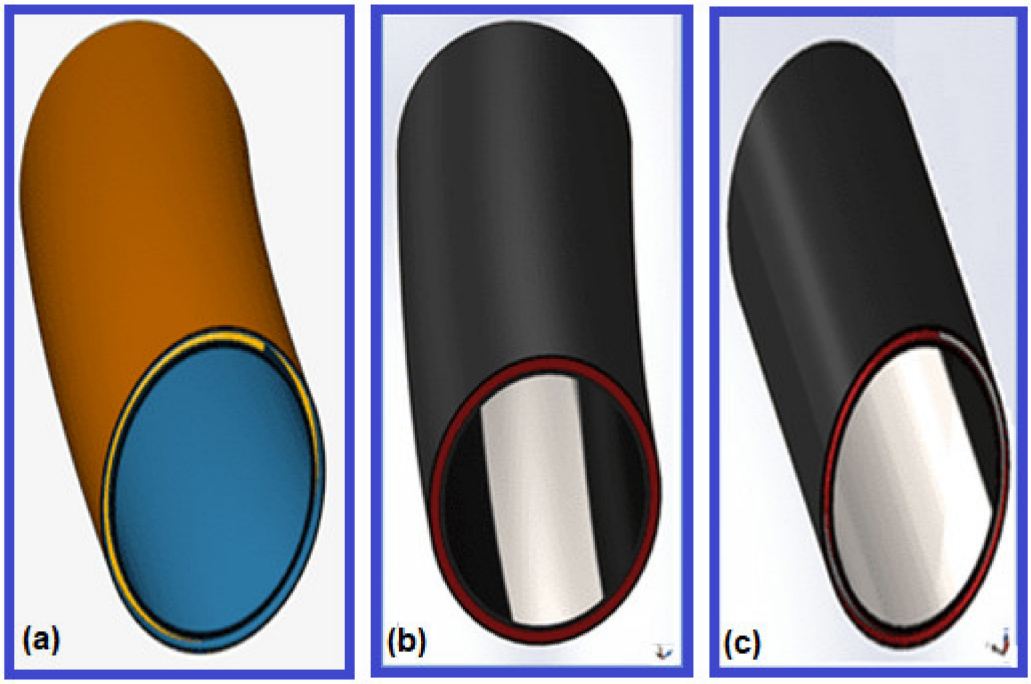

Figure 2. Reeling hose model showing (**a**) reeled section in Simscale OpenFEA, (**b**) reeled section in Solidworks, and (**c**) unreeled sections in Solidworks.

2.2. Methodology

In the local design, the hose geometry was generated in a CAD using Solidworks 2020. It was then modelled in ANSYS Structural version R2 2020 and ANSYS ACP Composites modules, as it had composites layers. Due to computational modelling challenges, the finite element model (FEM) was also run using Simscale OpenFEA online platform. The FEM results of the hose obtained from the local design were analysed to predict its mechanical behaviour. These analyses were performed by applying certain considerations to achieve the best results on the model. The first consideration was to simplify the model, while the second was to homogenize the model. The initial simplified model and the separate helix spring are shown in Figure 2a. The application of the FEM of the marine bonded hose involved the development of the marine hose model, the mesh generation, introduction of the properties and behaviour of the physical hose models, the introduction of the boundary conditions, the loadings (internal pressure, external pressure, and load cases), and the analysis and evaluation of results, as shown in Figure 3. The finite element analysis (FEA)

involved internal pressure, external pressure, and load case. Next, a tensile crush load on the spring reinforcement was also carried out, as stated in Sections 3.6 and 3.7.

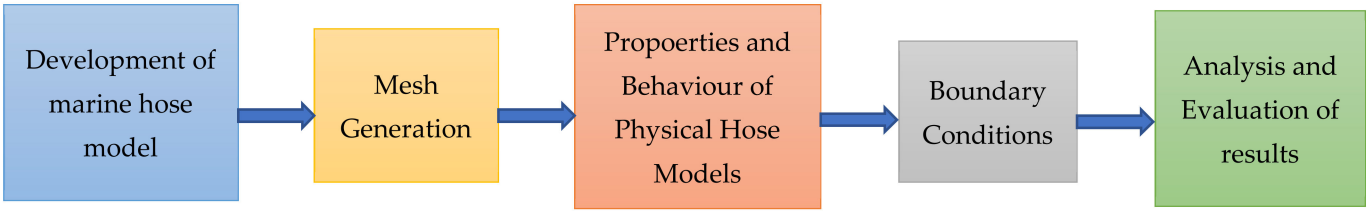

Figure 3. Methodology for the finite element model of the marine bonded composite hose model.

2.3. Material Properties

The material properties considered in this model for steel and composites are presented in Table 1. These material properties were chosen based on their high potential for application in flexible bonded pipelines. They demonstrate high potential based upon their complimentary properties, such as high strength, natural corrosion resistance, lightweight, and flexibility. The physics of the contacts considered were the bonded contacts perfectly held, without any slippage and no separation. For the composite layers, the hoop layers direction was defined as 0^o for the composite materials. Table 2 presents the layers and the material selections considered in this model.

Table 1. Material properties for steel and composites.

Material	Density (kg/m^3)	Young's Modulus (Pa)	Bulk Modulus (Pa)	Shear Modulus (Pa)	Compressive Yield Strength (Pa)	Tensile Yield Strength (Pa)	Tensile Ultimate Strength (Pa)	Poisons Ratio, v
Structural Steel	7850	2×10^{11}	1.6667×10^{11}	7.6923×10^{10}	2.5×10^{8}	2.5×10^{8}	4.6×10^{8}	0.3
Nylon PA6/6	1140	1.06×10^{9}	1.1778×10^{9}	3.9259×10^{8}	2.32×10^{9}	4.31×10^{7}	4.97×10^{7}	0.35
Nylon PA66-GF *	1360	6.82×10^{9}	7.5778×10^{9}	2.5259×10^{9}	3.45×10^{7}	1.39×10^{8}	1.49×10^{8}	0.35
CF (290GPa) +*	1810	2.9×10^{11}	2.45×10^{11}	9×10^{9}	5.7×10^{8}	4.2×10^{9}	6×10^{8}	0.3
Resin Polyester	1200	3×10^{9}	2.7174×10^{9}	1.1398×10^{9}	1.41×10^{8}	1.28×10^{8}	5.18×10^{7}	0.316

Details on the anisotropic material properties for the composites are from MatWeb, Granta, and Ref. [9]. * GF means glass-fibre-reinforced. +* CF means carbon fibre.

Table 2. Material consideration for reeled hose layers.

Layer	Liner	Main Plies	Filler	Helix	Holding Plies	Sub Cover	Breakers	Cover
Material	Structural Steel	Nylon 6/6 glass fibre reinforced (PA66-GF)	Nylon 6 (PA6)	Structural Steel	Resin polyester	Carbon fibre (290 GPa)	Resin polyester	Carbon fibre (290 GPa)

2.4. Marine Hose Layers

The marine hose structure is detailed within this model in order to make the simulation as realistic as possible. It is important to note that marine hose designs have more layers in reality. On the other hand, simplification was normally required without loss of generality (i.e., form) to achieve a successful numerical simulation. In this paper, it was a priority to investigate the use of the new composite materials implemented in these designs. Therefore, different composite plies were utilised in the model for the main and holding plies. The sub-cover and cover were to be made of structurally strong composites to add solidity to the structure. However, a key component to the design of this hose tubular is the steel structural helix embedded within the filler layers. This differentiates it from conventional marine

risers, pipe-in-pipe tubes, and reeled steel pipelines. The steel helix, as depicted in Figure 4, acts as a vital longitudinal reinforcement to the pipeline and is a critical component in the investigation of structural deformation behaviour, as a common fault in these hose-riser structures is helix rupture or delamination from its filling layer [86–89]. The helix also experiences deformation due to crush load of the spring against the reeling drum. Therefore, independent analysis of this layer is essential. The geometrical data of the layers for the marine hose models are presented in Tables 2 and 3.

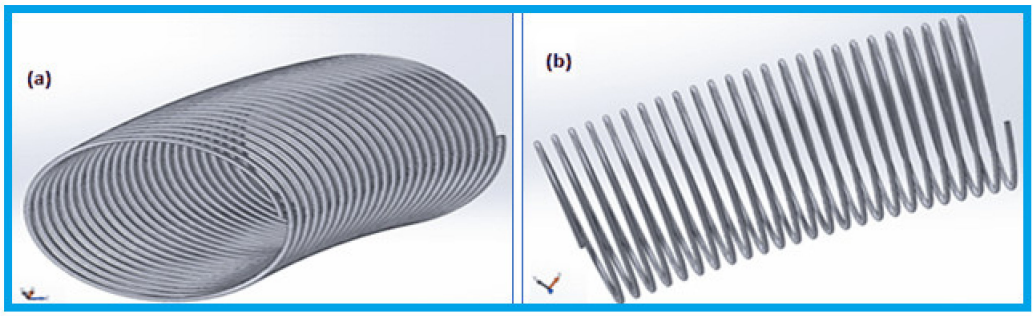

Figure 4. Helix reinforcement of the marine hose, showing (**a**) isotropic, and (**b**) side views.

Table 3. Marine hose model dimensions.

Layer	Inner Diameter (mm)	Outer Diameter (mm)	Thickness (mm)
Liner	488.95	493.95	5
Main ply 1	493.95	496	2.05
Main ply 2	496	498.05	2.05
Main ply 3	498.05	500.1	2.05
Main plie 4	500.1	502.15	2.05
Main ply 5	502.15	504.4	2.25
Main ply 6	504.4	506.25	1.85
Main ply 7	506.25	508.3	2.05
Main ply 8	508.3	510.35	2.05
Filler 1	510.35	517.35	7
Steel helix	517.35	545.79	14.22 **
Filler 2	545.79	552.79	7
Holding ply 1	552.79	554.84	2.05
Holding ply 2	554.84	556.89	2.05
Sub cover	556.89	559.39	2.5
Breaker 1	559.39	560.59	1.2
Breaker 2	560.59	561.79	1.2
Cover	561.79	564.29	2.5

Note: Radius of curvature of marine hose layer = 6.25 m; ** Pitch of helix's coil = 40 mm.

Dimensions were set for each layer, as illustrated in Figure 5. This setup was designed according to industry examples to represent the asset accurately. In practice, the composite 'main plies' are of varying angles, while the helix reinforcement layer is fully encased in a single filling layer. However, the present study's scope did not include details on the reinforcement angles. For this design, simplicity increased the ability to vary the simulations under different loading conditions. The material choices of the model demonstrate high variation of both metallic materials and composites. In a practical design, a bonded flexible pipeline utilises a mixture of both material categories for enhanced structural properties of the asset. There are various materials chosen for different layers of the model regarding the composite material choices. Steel was chosen as the metallic component of the model for the inner liner and reinforcement helix. Composite material choices included resin polyester, carbon fibre (290 GPa), nylon 6 (PA6) and nylon 6/6 glass-fibre-reinforced (PA66-GF). These materials have been validated in modelling composite risers and thermoplastic composite (TCP) pipes in previous studies [1,9,81].

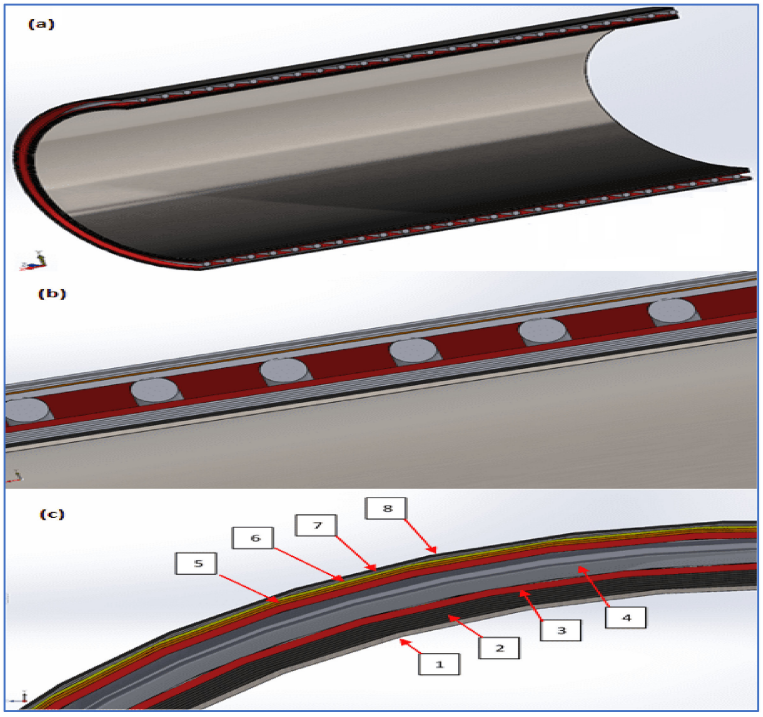

Figure 5. Cross-section through hose showing layers with the helix reinforcement in (**a**) open view, (**b**) closed view, and (**c**) labelled section of layers for the liner (**1**), main plies (**2**), filler (**3**), steel helix (**4**), holding plies (**5**), subcover (**6**), filler (**7**) and main plies (**8**).

The length of the hose in this model was 1 m long. It was modelled with filler layers whereby the helix was placed in-between fillers to sandwich the helix, rather than modelled within one filler layer. This was done for the simplicity of the model design when at the CAD stage to make construction easier while still providing satisfactory results in simulation. Both reeled and unreeled models were created with the same layering system to simulate a localised region of the pipeline, experiencing crush load from the reel drum. The reeled riser model was made with a radius of curvature of 6.25 m in order to correctly simulate the pipe being laid across the reel drum of diameter 12 m. Detailed below is the initial simulation material selection for the different layers. It is important to note that different plie angles were not applied at this stage, as the main aim was to obtain a working simulation to begin with. Therefore, the ply angles were all be considered to be unidirectional in the hoop direction.

3. Finite Element Model

The details on the finite element model for the MBCH are provided in this section.

3.1. Local Design

The finite element model was developed in ANSYS Workbench R2 2020. The details of the local design are presented in Section 2 and the other aspects, including the mesh details, boundary conditions, and design loads, are all in Sections 3.2–3.6. In this model, the failure criterion considered was the maximum stress criterion. The local design for the marine hose was based on beam theory [90–93].

3.2. Mesh Details

The meshing details for the first case of the reeled hose model recorded a total of 2.7 million cells comprising of 12,538 edges, 1,841,382 faces, and 923,798 nodes. The mesh selection was conducted using a fine mesh with 6.8 points in Simscale and 2nd-order elements. This gave good convergence results in this study. The mesh was developed using a global gradation rate of 1.22, and a small feature suppression of 1×10^{-5} m. The mesh

was simplified using this mesh case, as represented in Figure 6. Some comparisons were made using a hose model without helical spring. This model was also further simplified by collectively grouping the similar layers into one layer, i.e., main plies 1–8. The spring was also modelled separately, and not homogenised with the other hose layers.

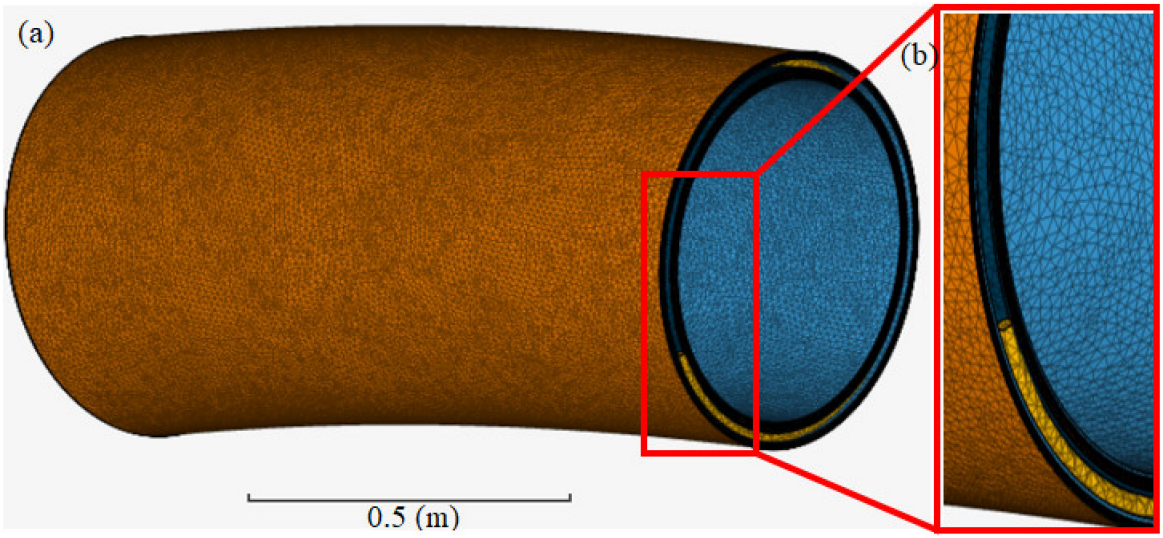

Figure 6. Mesh model for the marine hose in Simscale Platform showing (**a**) the full mesh model and (**b**) the magnified mesh detail.

3.3. Boundary Conditions

Different boundary conditions were considered based on the operation. For the pressure loading cases, fixed ends were considered, but when the torsional motions were induced, the loads were induced at one end that was set free. Fixed supports were applied to all faces at the fixed ends of the pipeline such that it was locked in place. The reinforcement helix was fixed at the end of the spring.

3.4. Design Load Conditions

This marine hose model's local design followed the design standards for bonded pipes in industry specifications [94–97]. The following loading conditions were applied to simulate burst, collapse, tension, and crushing, as given in Table 4. The results of total deformation, shear stress, equivalent stress, and elastic strain were obtained using the simplified model. The hose structure was subjected to both internal and external pressures during the operation conditions. External pressures occurred due to the dynamics of the wave motion surrounding the hose accompanied by varying hydrostatic forces, varying with depth. However, the hose also had to operate under significant internal pressure to transport the targeted fluid while the production/drilling asset was extracting or transferring fluid. These internal fluids may be gaseous or liquid, with varying levels of viscosity. With an increase in viscosity, an increase in operational internal pressure was required to move the object fluid inside the hose. An internal pressure of a magnitude of 9 bar, as depicted in Figure 7, was applied to the liner inner face as a realistic starting operating pressure. Additionally, the standard gravitational force was applied to the pipeline to represent the self-weight of the marine hose.

Table 4. Design load conditions.

Design Load	Loading Description
Burst (Internal Pressure)	Burst test at 2.0 MPa, 3.5 MPa and 5 MPa
Collapse (External Pressure)	Collapse test at 4.5×10^5 Pa, 7×10^5 Pa, 9.5×10^5 Pa, 1.26×10^6 Pa
Crushing Load	The crush load was an external pressure of 2.1×10^5 Pa

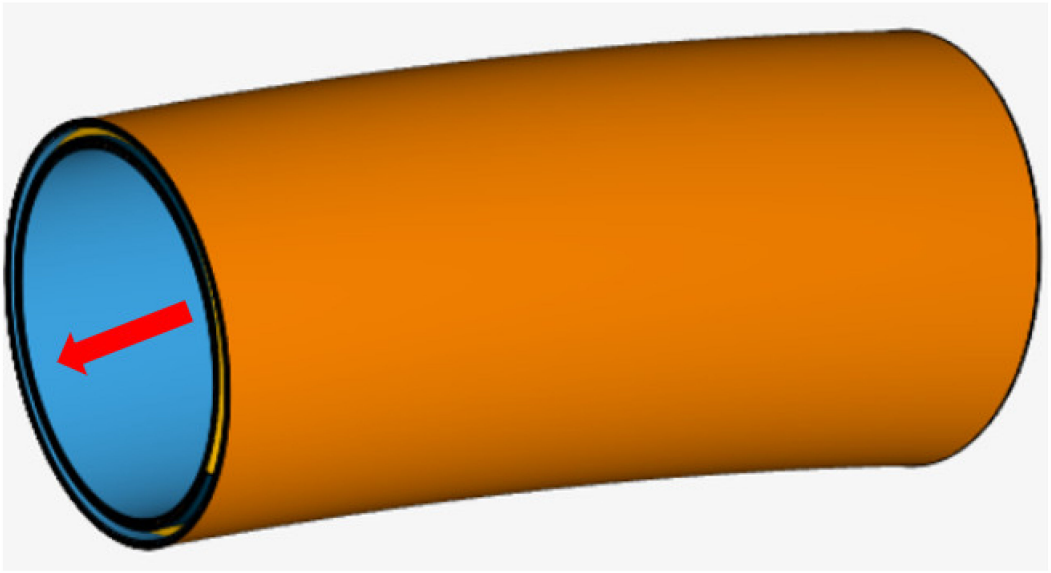

Figure 7. Internal pressure load applied on the offshore hose in Simscale Platform.

3.5. Helix Compression/Tension

This model was created with similar dimensions to industrial designs. The helix was of a short pitch, 40 mm, and the diameter of about 14.22 mm. The material chosen for this simulation was steel, as stated previously. The model used for this simulation is depicted in Figure 8. An external pressure of 2000 Pa was applied perpendicularly at each end of the helix to the faces of the ends of the helix. This was done purely to observe the general mechanical behaviours when the entire helix is subject to uniform compressive force at each end. Lower pressure was applied upon the model to observe the trend on this hose's helix being investigated. The hose section was loaded from both ends. This was to observe its response from its own weight or other connecting sections pushing against the hose section. It should be noted that the spring could have been modelled by selecting an equivalent elastic support condition or even a virtual spring in ANSYS, making the model substantially more efficient. These spring loads may be considered in both tensile and compressive directions. However, the spring was fully modelled because the study aim was to investigate the spring behaviour so that spring load and the number of spring layers (one or two helix springs) could be factored into the conceptualisation of the model.

3.6. Crush Load on Helix Spring

During operation, the marine hose structure experiences compressive loading from other surrounding spooled sections, the reel drum itself or a combination of both. These crush loads will be consistently applied throughout the hose's life span. With continually repetitive loading of this nature, this could lead to potential fatigue cracking of the helix structure. As the helix is compressed, the shape begins to ovalise and offer a high potential for cracking. As a result, it was deemed imperative that this loading case be analysed via simulation to better understand the resulting mechanical behaviours of the helix due to crush loading. The crush load, as depicted in Figure 9a, is necessary as the helix can induce either layer delamination or reinforcement helix rupture. However, details on the delamination are not included in the scope of the present study. The OCIMF industry guidelines [98,99] do not specify crush load for helix spring specification. However, the GMPHOM OCIMF 2009 [99] determines guidelines for a marine hose section, without specifics for the helix reinforcement. It defines a shorter hose section as the test profile with a nominal length of 500 mm placed on a flat surface with supports. The test criteria further prescribed for the hose crush load apply a crushing load by utilising a flat beam profile of 500 mm lengthwise and 400 mm widthwise. This study proposes a longer profile for the helix, as shown in Figure 9a,b. Table 5 presents the parameters considered in developing the

helix geometry considered in the crushing test. The helix models have the same dimensions and materials as used in both ANSYS and Simscale simulations. In this model, the helix was not modelled in a reeled state, as it was formerly, but in a straight and unreeled layout. This helix was then modelled between two steel plates of the same dimension. These metal plates were then bonded to the helix structure, and external pressure was applied to each plate directed in opposite directions as each other in order to replicate a crushing load, with respect to (w.r.t) X-X and Y-Y planes, as depicted in Figure 9a. The simulation setup is depicted in Figure 9b.

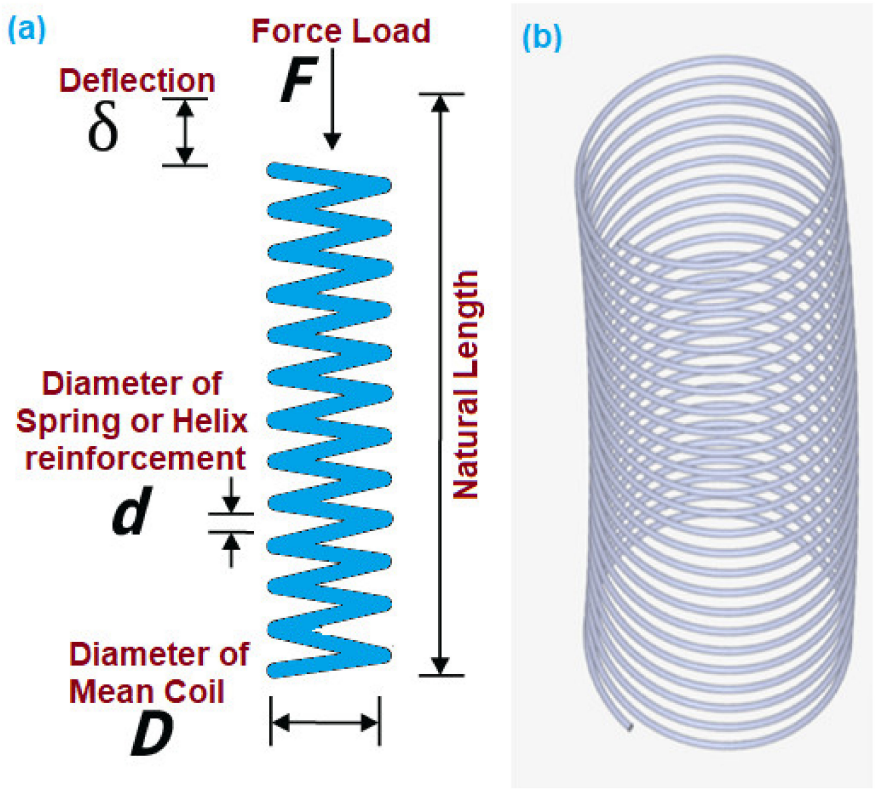

Figure 8. Schematic, showing (**a**) notation for helix spring, and (**b**) the reinforcement helix model.

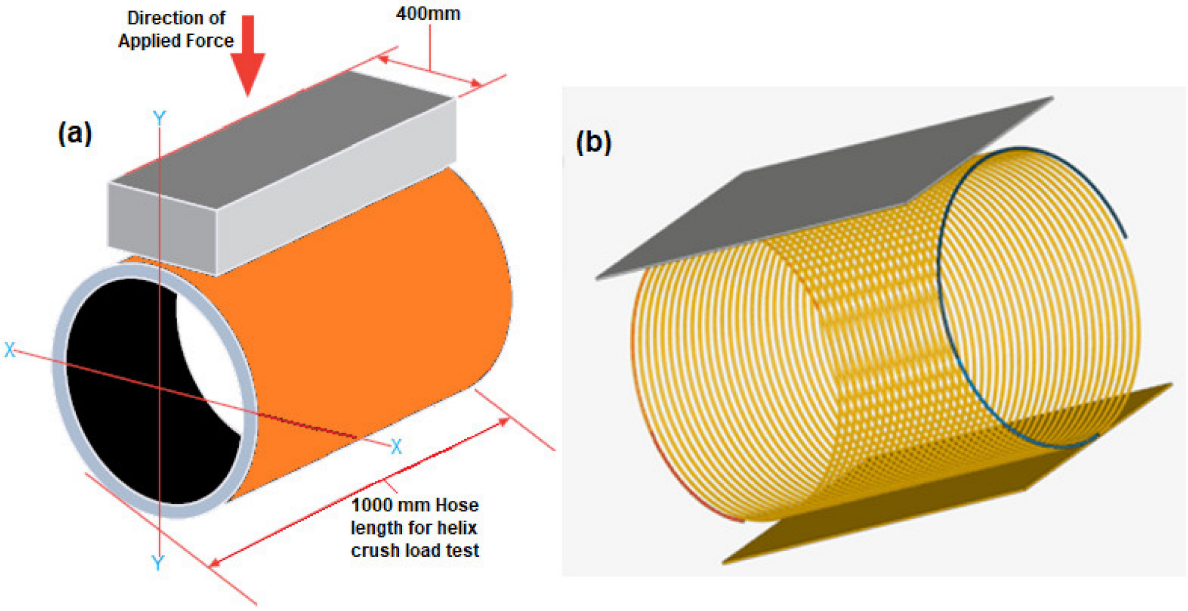

Figure 9. Reinforcement helix model compression, showing (**a**) hose crush load and (**b**) FEM of spring.

Table 5. Parameters for marine bonded composite hose (MBCH) and helix reinforcement models.

Parameter	Value	Unit
Hose Nominal inner radius	250	m
Outer radius	294	mm
Length of Hose model	1000	mm
Mean Radius of helix reinforcement	284	mm
Diameter of helix reinforcement coil	12.7	mm
Pitch of helical reinforcement	36	mm
Total number of coil turns	41	-
Height of helix reinforcement	1500	mm
Width of helix reinforcement	1200	mm

3.7. Validation

To understudy this model, the results of this investigation were compared using a composite riser with 18 layers of composite plies [9]. As observed in Table 6, the factor of safety (F.S) values obtained for the composite plies and the steel layer were 9.2 and 7, respectively. The FEM's strain results from the present study were profiled by a comparative validation method using a similar hose study but on stiffened marine hoses [76]. The present model is a marine hose without stiffened layers considerable for submarine hoses and floating hoses, while the study by Gao et al. [76] is a marine hose with a steel-stiffened layer considerable for dredging hoses. Thus, this study was not comparable due to the differences between the material and the hose's purpose. Both did not have a very close relationship in the strains because the type of marine hoses differed. However, the validation method is acceptable as it observed that the strains have similar intercepts in Figure 10. It gives a linear equation obtained using the line-fitting function on the data expressed in Equation (1). Moreover, the study showed that the axial strain is almost directly proportional to the internal pressure, as axial strain increased as burst load increased. However, note that a detailed validation is recommended in further studies, including analytical or experimental modelling of the marine hose.

$$y = 0.0007x + \left(6 \times 10^{-5}\right),\ R^2 = 0.9966 \tag{1}$$

for the validation of the spring model, an analytical method is considered. Using the analytical spring formula presented in [100] for the analytical relationships from Wahl's spring equations, the stiffness of the spring can be computed. Using these formulations, the spring constant, k obtained is k = 3.62 N/mm. This was used to validate the simulation result of the helix reinforcement in Section 4. Some theoretical formulations used are given in Equations (2)–(4), where d is the spring wire diameter, D_{outer} is the spring outside diameter, G is the material's shear modulus, v is the material's Poisson ratio, E is the material's Young's modulus, and nI_a is the active coils or turns on the spring.

$$D = D_{outer} - d \tag{2}$$

$$G = \frac{E}{2(1+v)} \tag{3}$$

$$k = \frac{Gd^4}{8D^3 n_a} \tag{4}$$

Table 6. Comparison on study comparing factor of safety (F.S).

Model Particulars	F.S of Composite Plies	F.S of Steel Layer
Present Study	9.2	7

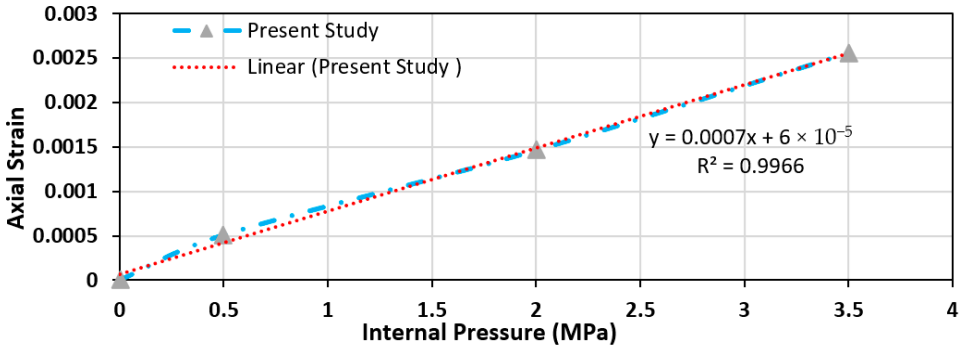

Figure 10. Validation plot for axial strains against internal pressure.

4. Results and Analysis

This section provides a concise and precise description of the numerical results, their interpretation, the observations made, and discussions drawn on this study.

4.1. Results of Helix Reinforcement

The FEA results on helix reinforcement presented in Section 3 are discussed here. In Figure 11, it can be observed that the spring has different tensile and compressive behaviour. Two spring helix reinforcement models were investigated, which are made of stainless steel and composite material, respectively. However, only the results of the stainless-steel model for the helix reinforcement were considered in this paper. All the models discussed in this section were set-up and run to completion, utilising the Simscale online virtual FEA tool. The models were designed to simulate and analyse multiple loading conditions of marine reeling bonded flexible riser pipelines, utilising composite material and helical reinforcement layers. For the models demonstrated in Figure 11, an internal pressure of 2.5 MPa was applied to observe the resulting behaviours of the model. The factors to be observed were strain magnitude, von Mises stress, and displacement. As expected, with the internal pressure acting uniformly throughout the hoseline section, the force was greatest at the inner face of the pipeline liner. The areas experiencing the greatest force per unit area had higher magnitudes of profiled parameters. Moreover, the effects of this should gradually decrease throughout the model layers from the internal face of the liner.

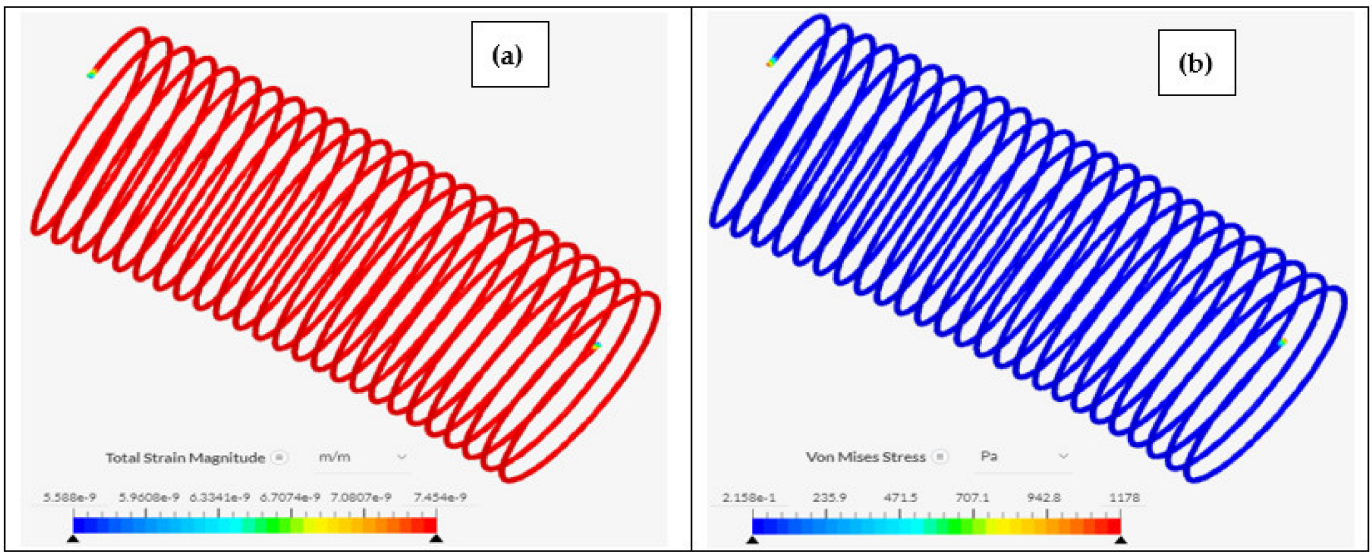

Figure 11. Reinforcement helix for the bonded flexible hose under loading, showing (**a**) strain magnitude, and (**b**) von Mises stress, as carried out in Simscale OpenFEA.

4.2. Results of Crush Load on Helix Spring

For the crush test displayed in Figure 12, the crush load was an external pressure of 2.1×10^5 Pa exerted on the flat planes. The stainless-steel model was selected as it was observed that it performed better in a pre-analysis. From the crush load test, the deformation, strain, and stress results are presented. The present study investigated the crush load only on the spring reinforcement. It can be observed in Figure 12c,d that the end of the spring attracted the maximum deformations and stresses. Thus, proper attention had to be given to it during the design and manufacture of marine bonded hoses. A detailed crush load effect is recommended to investigate the effect of couplings and end-fittings of marine hoses when in contact with the FPSO body or reeling drum. Typical nonlinear analyses of spring models with similar failure mode analysis of hoses are in [48–51,82].

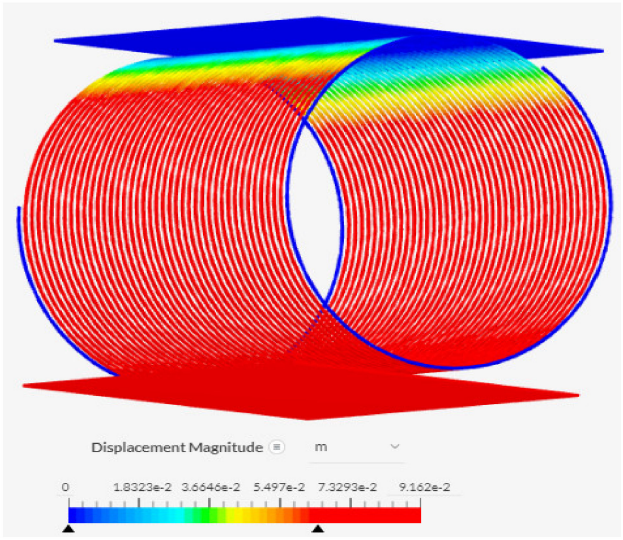

(a)

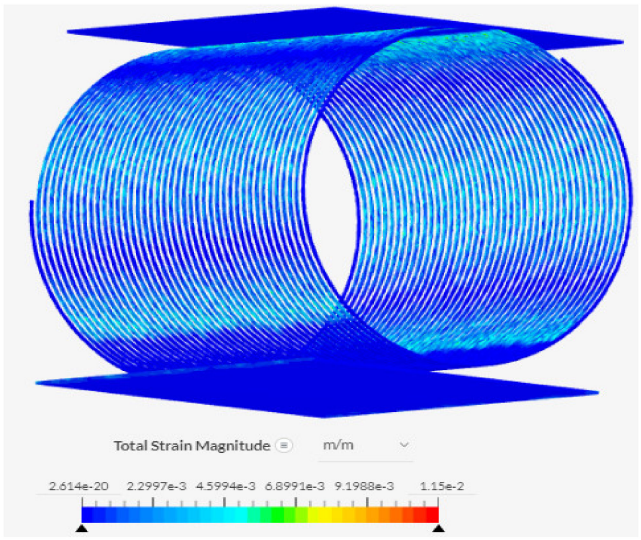

(b)

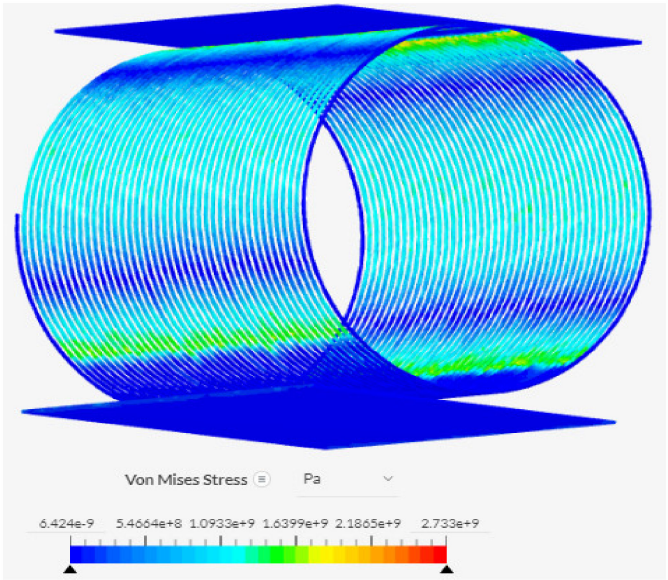

(c)

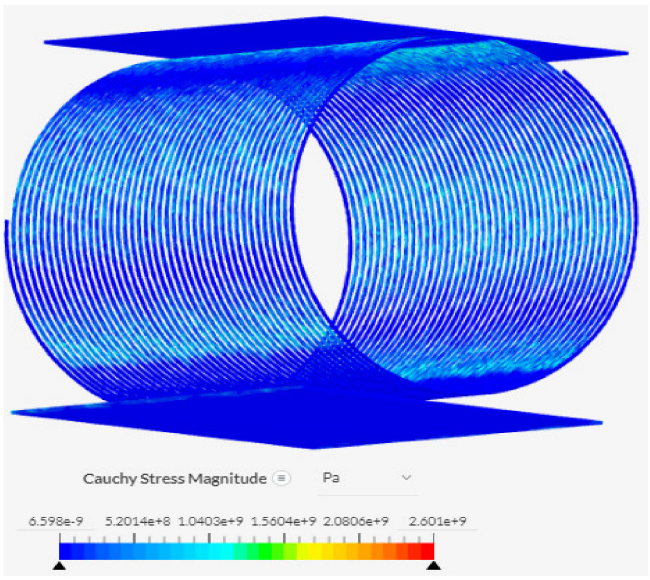

(d)

Figure 12. Compression on reinforcement helix for the bonded flexible hose, showing (**a**) deformation, (**b**) total strain magnitude, (**c**) von Mises stress, and (**d**) Cauchy stress using Simscale.

4.3. Results of Helix Spring Beam Model

A significant force that is involved in the reeling process is the crush load experienced by the pipeline crushing against the reel drum under tension and its own weight. Although unlikely to be crushed uniformly, a simulation of a collapsing case of the pipeline was carried out. In the reeling process, this could perhaps be experienced to a certain extent due to the possible build-up of pipeline sections stacked on top of each other, either during storage or through piled reeling on the reel drum. Two different modelling methods were considered to investigate this mechanical behaviour. The first is the beam model while the second is the hex-solid model. The effect of compression from a crushing load can be observed on both the models in Figures 13 and 14. As seen on Figure 13, there is a relationship between the force reaction per time obtained using the beam model and the hose helical spring reinforcement model. Moreover, the linear relationships in Equation (5) and the polynomial relationship in Equation (6) show that the spring beam model can have a linear and a nonlinear relationship. As such, it could have issues with damping the helical spring reinforcement even during crush load application, as shown in Figure 13.

$$y = -0.1297x + 0.1481,\ R^2 = 0.9725 \tag{5}$$

$$y = -0.0084x^2 - 0.0451x + 0.0057,\ R^2 = 0.9998 \tag{6}$$

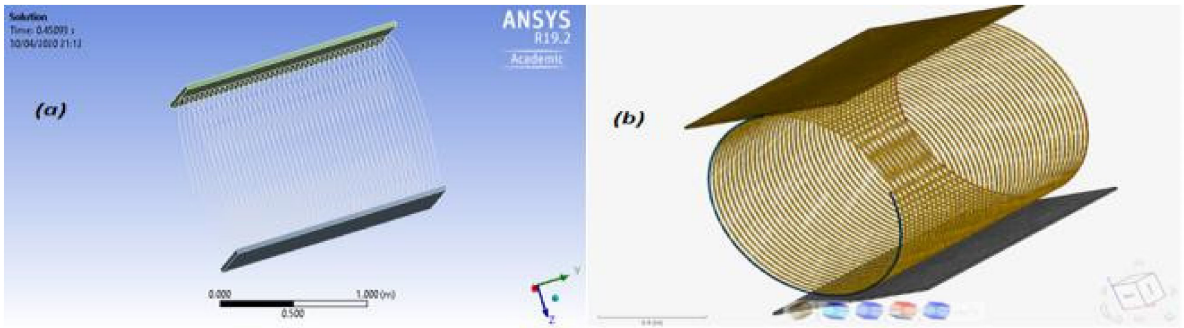

Figure 13. The offshore bonded composite hose for the (**a**) beam model in ANSYS Structural R19.2 and (**b**) hex-element model in Simscale OpenFEA.

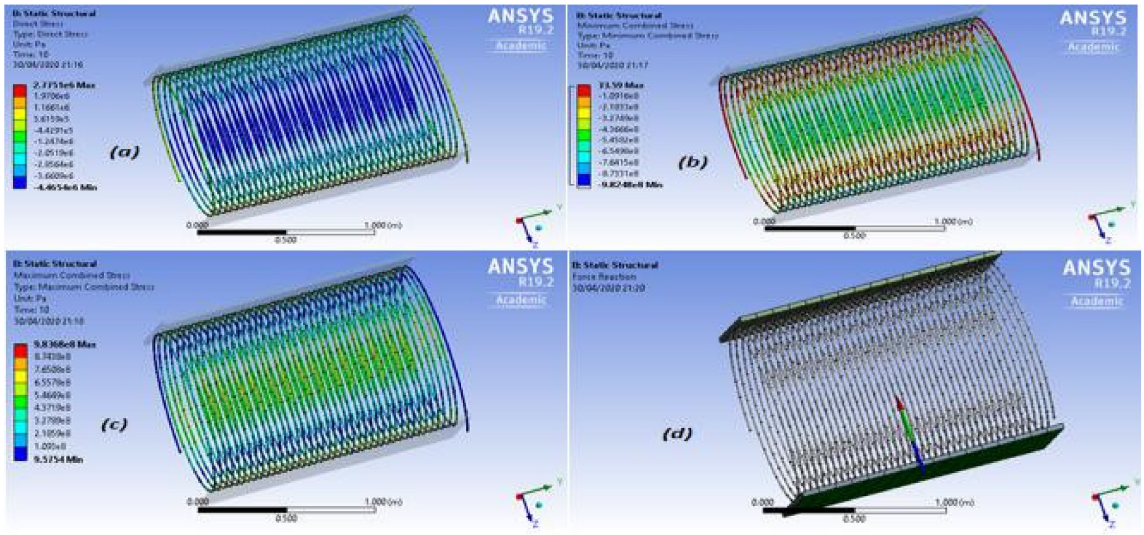

Figure 14. Helical spring beam model of the offshore bonded composite hose, showing (**a**) direct stress, (**b**)minimum combined stress, (**c**) maximum combined stress, and (**d**) force reaction.

Thus, the second model used had a much better representation of the stress behaviour of the spring in Figure 14. It shows areas of high stress magnitude which must be considered when laying the reinforcement or embedding it into the offshore bonded composite hose. Figure 15 presents the plot from the dynamic analysis of the beam model. The analysis is time-dependent, and the supporting plates were fixed. Both Equations (5) and (6) have spring meaning when compared to the spring equations presented in Appendix, as proposed earlier by Wahl [100]; however, this holds for steel materials. Further studies are recommended using sustainable spring materials such as high strength composites.

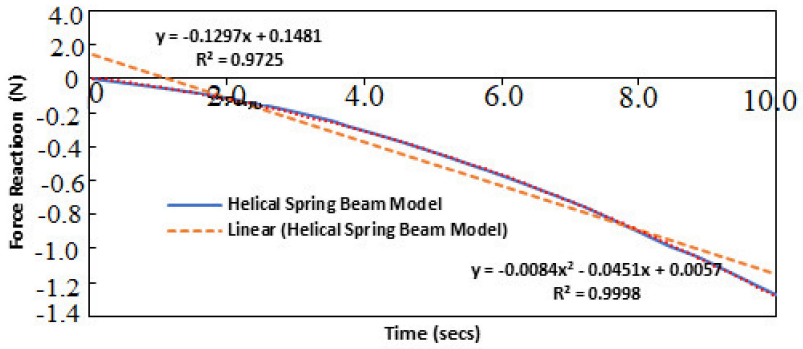

Figure 15. Helical spring beam model showing the force reaction of the marine bonded composite hose.

4.4. Results of Internal Pressure

The results obtained from the burst case on the reeling hose in the local design are presented in Figures 16–18. Three different ranges were considered based on previous predictions for the internal pressure, these are: 2.0 MPa, 3.5 MPa and 5 MPa. With the internal pressure acting directly at the innermost face of the liner of the hoseline, the results demonstrated maximum magnitudes of all monitored factors at this layer.

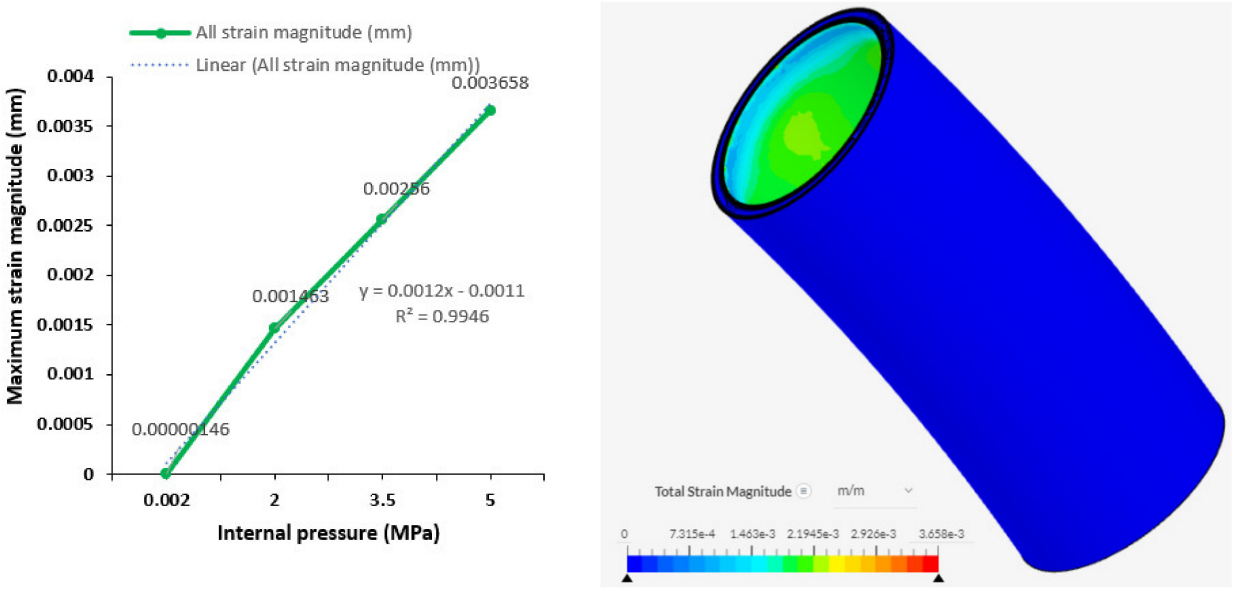

(**a**) (**b**)

Figure 16. Strain Profile of the bonded flexible hose under internal pressure, showing (**a**) the maximum strain magnitude under internal pressure at 5 MPa, and (**b**) Total strain magnitude of the hose.

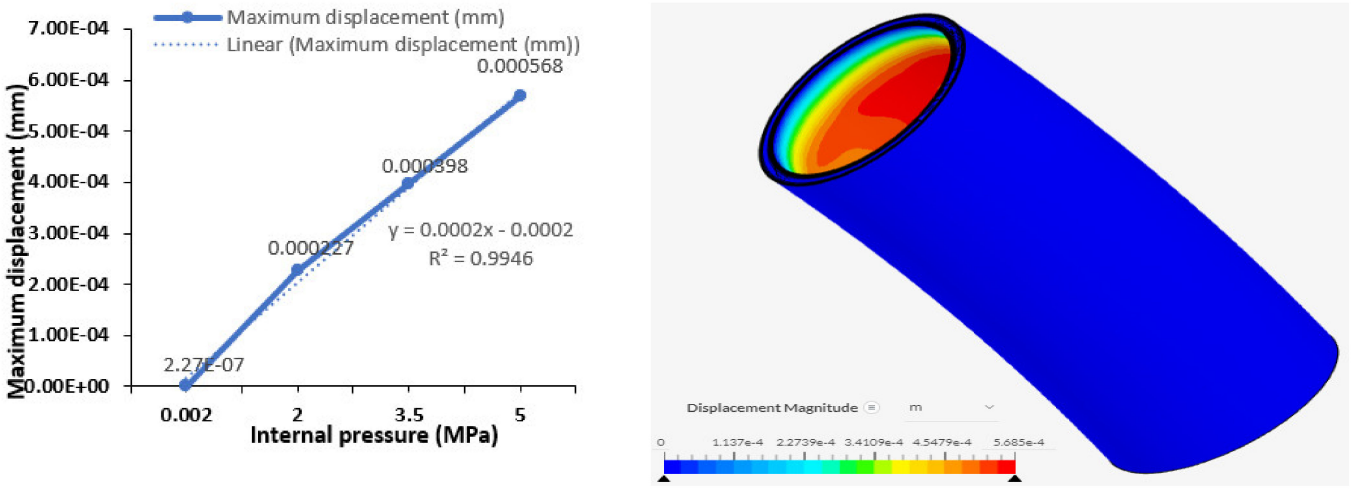

(**a**) (**b**)

Figure 17. Deformation Profile of the bonded flexible hose under internal pressure, showing (**a**) the displacement profile under internal pressure at 5 MPa, and (**b**) Maximum displacement of the hose.

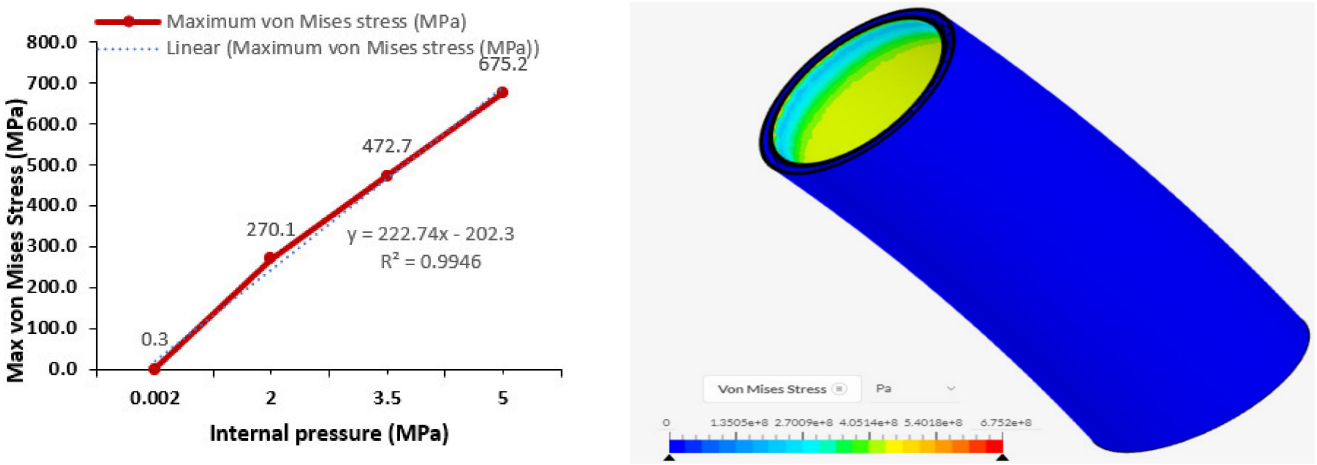

(**a**) (**b**)

Figure 18. Stress Profile of the bonded flexible hose under internal pressure, showing (**a**) the von Mises stress profile under internal pressure at 5 MPa, and (**b**) Maximum von Mises stress of the hose.

Displacement demonstrated the highest magnitudes at the inner liner, with some distance from the end of the section. Although the values displayed would be realistic values experienced, this also shows the behaviour of the marine bonded composite hose model under extreme and operational conditions. It should also be noted that the same boundary conditions were also applied to this burst case to obtain the results presented.

However, the results of this case are significant in identifying the pipeline behaviour mechanically to a crushing load. Generally, composite riser pipelines and offshore reeling hoses fail in service, before their theoretical lifetime, due to the mechanical fatigue experienced by the pipeline crushing against the reel drum. As given in Figures 16–18, the plots have a curve fitting of linearity given in Equations (7)–(9), showing a relative increase as the pressure increases, and thus showing an effective material model. Moreover, this study demonstrates the location of the maximum stresses and deformation occurrence when the structure is constricted. The results in Figures 16–18 show that the reinforcement layer would have certain areas likely to have earlier fatigue if the extreme loadings cause the structure to fail, or that possibly indicate the areas of deformations. It is recommended that

there be more reinforcement along the locations of these primary areas of delamination from the filler layer surrounding the reinforcement.

$$y = 0.0002x - 0.0002,\ R^2 = 0.9946 \quad (7)$$

$$y = 227.74x - 202.3,\ R^2 = 0.9946 \quad (8)$$

$$y = 0.0012x - 0.0011,\ R^2 = 0.9946 \quad (9)$$

Magnitudes of displacement decreased severely with radial distance from the inner liner. This results from the liner itself absorbing the highest magnitude of force per unit area, with the following composite plies experiencing less from this force with distance from the displaced liner. Following similarly are results of strain magnitude as well as both principal and von Mises stress. The highest magnitudes occur at the inner liner face and, again, they severely decrease with radial distance. However, it is noteworthy with regards to the von Mises stress that it can be demonstrated that at the very edges of the ends of the section are small areas demonstrating the highest magnitudes of stress, at around 270 MPa. These small areas demonstrate areas of high potential for potential cracking or fatigue, especially at higher operational pressures or possible uncontrolled pressure spikes. The liner at the very ends of the section should be an area of close monitoring if the asset exhibits this behaviour under internal pressure. In industry, ruptures and cracks have been witnessed at the end connections of these flexible risers, and this sort of mechanical behaviour may potentially demonstrate why this occurs. It is recommended that the reeling be done under operational pressure and not design pressure, as the study shows that design pressure could be high.

4.5. Results of External Pressure

From the collapse case on the reeling hose in the local design, the results obtained are presented in Figure 19. Three different ranges were considered for the external pressure, these are: 4.5×10^5 Pa, 7×10^5 Pa, 9.5×10^5 Pa, and 1.26×10^6 Pa. Upon observation of the post simulation images and graphical results it was determined that the results were as predicted. With an increase in compressive force comes a proportional increase in all factors monitored. As given in Figure 19a–c, the plots have a polynomial curve fitting given in Equations (10)–(12), showing a relative increase as the pressure increases, and thus showing an effective material model. In addition, wrinkling was observed on the body of the offshore bonded composite hose along the arc length.

Based upon the post-simulation images, maximum deformation occurs at one half of the reinforcement coil structure, with a stark contrast in magnitude in the opposite section. Thus, this demonstrates the effect of ovalisation on the helix under crushing load, as observed in Figure 19d. Maximum stresses occur in a symmetric pattern, with the most severe distribution of stress demonstrated in three areas of the helix. This observation could suggest likely sites of the helical structure that show the highest potential for fatigue and microcracking, leading to the eventual rupture observed in real industry projects.

$$y = -0.0084x^2 - 0.0451x + 0.0057,\ R^2 = 0.9998 \quad (10)$$

$$y = -0.0084x^2 - 0.0451x + 0.0057,\ R^2 = 0.9998 \quad (11)$$

$$y = -0.0084x^2 - 0.0451x + 0.0057,\ R^2 = 0.9998 \quad (12)$$

The external pressure has an impact on the walls of each layer differently for the normal stress and the equivalent von Mises stress. In view of that, such locations need to have thicker external liner material or increase the coefficient of friction in the bonding contact. It can also be observed that the ends that had been fixed have high stress profiles. As such, it is recommended that highly reinforced ends be used at such ends to offset the high collapse pressure, such as the helix profile in Figure 8.

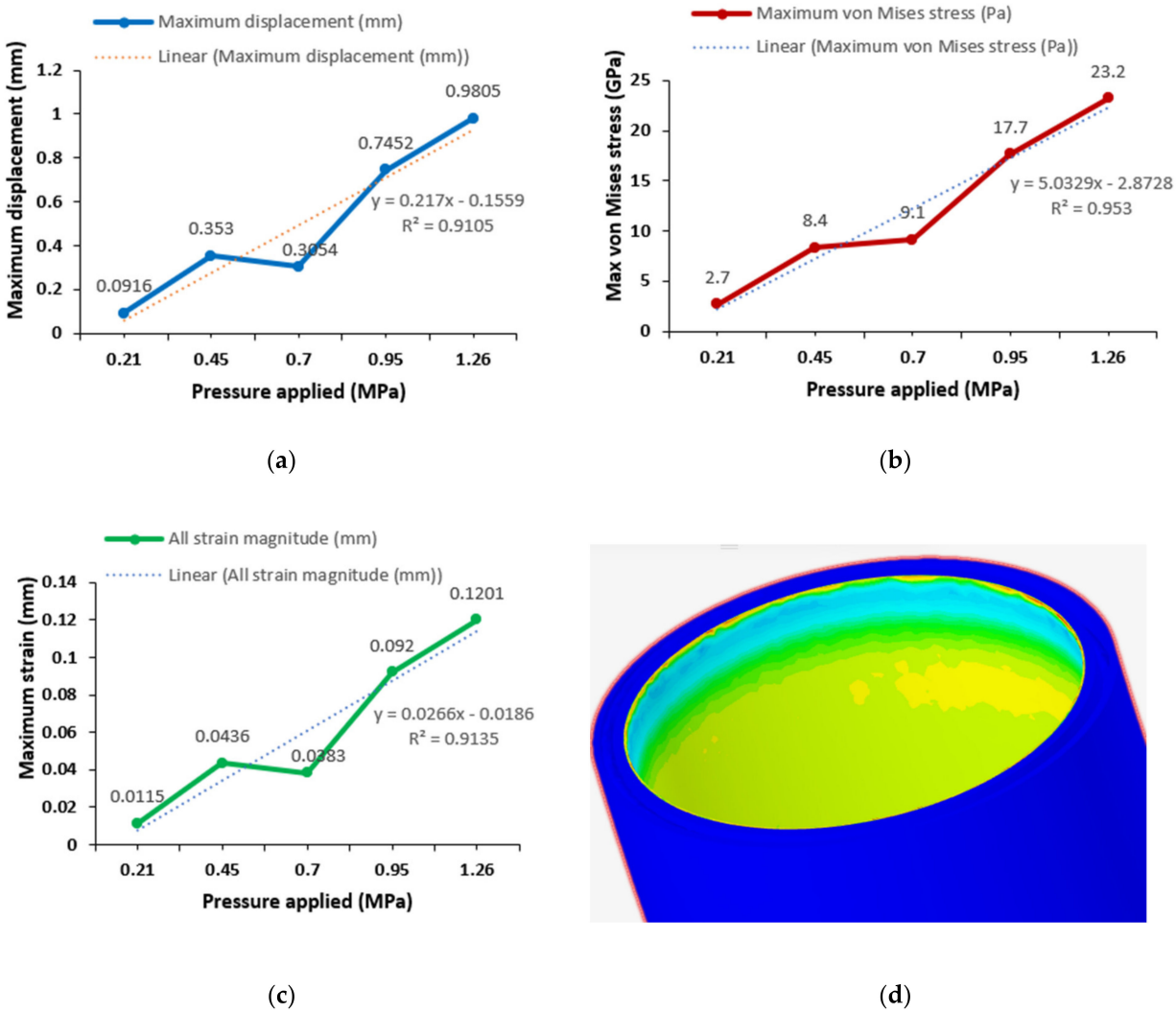

Figure 19. Profile distribution of Bonded flexible hose under external pressure showing (**a**) Deformation (**b**) Max von Mises stress, (**c**) Max strain magnitude, (**d**) Section of Von Mises Stress (VMS) profile.

4.6. Discussion of Results

The local analysis for the multiple layers simulated yielded useful results, demonstrating key areas of the internal pipeline structure that would be subject to the highest magnitudes of stress and deformation. The bursting case simulation results demonstrated how the pipeline would act under increased internal pressure as well as operational pressure. The simulation yielded expected results that coincide with the observations made in the literature when controlled burst tests were performed on the pipeline. In these tests, it was demonstrated that the pipeline structure failed due to open mode tearing of the structure with fast fracture. The results of the simulation showed areas of maximum deformation at the points of maximum curvature of the pipeline. With the pipeline already being in a reeled state, it provides an area of maximum stress concentration at the area of maximum curvature, indicating that this region of the pipeline section is most likely to fail first. A combination of tension, hoop stress from internal pressure, and increased deformation of the pipeline in this region demonstrates the optimal conditions of fracture of the pipeline materials. It can also be seen in deformation cases of extreme pressure that the internal reinforcement helix can be seen to bulge outwards, through the covering layers on top of the helix. This could indicate that as the pipe structure expands due to pressure the helix acts as a further source contribution to the actual opening mode tear, causing the surrounding layers to be stretched further as the helix expands resulting in increased

localised stress on the materials in question. Regarding the equivalent von Mises stress and normal stress results, it can be noted that higher magnitudes of stress can be seen to occur at the ends of the pipeline section. This result could be due to the pipeline's bulging motion. Thus, the ends should be reinforced with reinforced hose end. As the layers of the pipe expand at the area of maximum curvature, there will be an increase in tension in the structure as the layers are stretched, therefore resulting in increased stress at the end joints of the section. This indicates an area with increased likelihood of failure.

The simulation of the case of collapse of the pipeline, as already mentioned, was the first step in replicating a crushing load applied to the pipe section. Crush loading is a recent suggestion for the reason behind the fact that the actual in-service lifetime of composite reeled riser pipelines is significantly less than predicted. The results, alike for the bursting case, demonstrated key areas of the structure that could be cause for concern regarding increased likelihood of failure. Areas of maximum magnitudes were identified from the deformation profiles, which are also at the points of maximum curvature. It can also be noted that significant deformation can be shown at the inner liner, with internal bulging effects being demonstrated by the external layers surrounding it. The results obtained for the equivalent von Mises stress are useful for identifying areas of high magnitude. It was demonstrated in the results that the ends of the section are areas which seem to experience a higher magnitude of stress, similar to the results for the bursting case. This seems to be a reoccurring trend for both cases, therefore indicating that the end-to-end sections of the pipeline are an area of the section which should be monitored closely for fatigue analysis. Moreover, results for normal stress show a similar pattern as was shown in the previous bursting case, which also follows similar trends of the equivalent stress. Normal stress shows maximum magnitudes at the ends of the pipe section, further highlighting the ends of the section as being areas of increased likelihood of mechanical fatigue. Additionally, the results obtained from the collapse case in Section 4.5 also demonstrate how stresses are carried on the steel reinforcement layer alone. These results can be useful in replicating crush loading of the section on the helix, which can lead to the observed results of helix delamination from its filling layer or even rupture. Deformation results follow similar trends to those obtained in the burst case, with highest magnitudes being experienced at the area of maximum curvature of the section. Normal stress shows an almost uniform application throughout the helix structure and equivalent von Mises stress experiencing uniform application on all areas, except the very ends of the section.

5. Concluding Remarks

A finite element model of a bonded marine hose has been presented based on local design. The novel material model was developed with the material properties presented in Section 2. It was then used to investigate different design loads on the tubular structure developed. The meshing details, the boundary conditions, and the loads applied were discussed in Section 3. The application of the local design using a small section was to ensure less computational time and resources. This study presents the novelty of the local design and material modelling of marine bonded hoses with improved modelling techniques for marine composites in the oil and gas industry. Some recommendations were made on other modelling methods to consider in further study. Moreover, some areas of the designed hose were identified for further studies and optimisation to achieve a longer in-service life span.

The model highlights include: a novelty in the material modelling for the finite element modelling of marine hoses, used in local design. This concept was applied on flexible risers and pipelay analysis. This proposed method saves computational resources, is cost-effective, and has high accuracy. Extensive local design was also carried out on the hose model for reeled and unreeled sections. The second novelty was the study of the effect of compression load on marine hoses. In reality, some loadings originate from the vessel load response and the effect of fluid content density on marine hoses. Thirdly, application of composites on the multi-layered bonded structure was considered in this study. Fourthly,

there was some novelty in the crush load analysis on helix spring reinforcement of reeling hose, and combined loading on the reeling hose. Lastly, the model presents the behaviour of the bonded tubular pipe under pressure loads using design pressures and the bending scenario by analysing the deflections under burst and collapse loads.

From this study, the following conclusions and recommendations may be drawn:

1. The internal pressure and external pressure tests are very important aspects of the design of the marine bonded hoses. It was observed that the higher the pressure, the higher the von Mises stresses, maximum strains, and maximum deformations on the reeling hose, as presented in Section 4. However, detailed study is recommended based on combined loading and the effect of the composite materials in the layers.
2. Based on the study of the reeling hose operation, some deformations were observed in the structure. However, this can be minimised by increasing the reinforcement of the marine hose, by using lighter materials with high strength–weight ratio, such as composites, or by applying the hose hydrodynamic loads. It is also recommended that the reeling be done under operational pressure and not design pressure, as the study shows that design pressure could be high. It is also recommended that an explicit code be used which runs better for simulating higher failure conditions in further studies.
3. The crush load was a significant part of the study as it showed the behaviour of the helix spring reinforcement under compression. The spring material performed well as stainless steel, however further studies should consider other spring coil materials like composites. Secondly, further study is recommended on the detailed crush load based on different materials and hose layer delamination.
4. Based on the result on the helix reinforcement, it is important to optimise the hose model and investigate further on the helix. The results of the study also showed that the strains along the hose sections are reflected from the helix reinforcement.
5. In reality, based on oil field operation, the crush load analysis of the reeling hose section will consider HEV coupling along the reeling hose string. A detailed crush load effect is recommended to investigate the effect of couplings and end-fittings of marine hoses when in contact with the FPSO body or reeling drum. In addition, further research is also recommended on the reeling process under transient mode in the FEA, as well as the global design of the marine bonded hose under marine operations like reeling.

Author Contributions: Conceptualization, C.V.A., C.C., F.W., A.C.O. and J.Y.; methodology, all authors; software, C.V.A., C.C., H.O.B., F.W., Z.G., X.H., A.C.O. and J.Y.; validation, all authors; formal analysis, all authors; investigation, C.V.A., C.C., H.O.B., F.W., Z.G., X.H., A.C.O. and J.Y.; resources, C.V.A. and J.Y.; data curation, all authors; writing—original draft preparation, C.V.A. and C.C.; writing—review and editing, C.V.A., C.C., H.O.B., F.W., Z.G., X.H., A.C.O. and J.Y.; visualization, all authors; supervision, C.V.A., J.Y., X.H., A.C.O. and F.W; project administration, C.V.A., J.Y., X.H. and F.W.; funding acquisition, C.V.A., J.Y. and F.W. All authors have read and agreed to the published version of the manuscript.

Funding: The funding support of the Department of Engineering, Lancaster University, UK, and the Engineering and Physical Sciences Research Council (EPSRC)'s Doctoral Training Centre (DTC) is highly appreciated. In addition, the funding from the Overseas Postgraduate Scholarships by the Niger Delta Development Commission (NDDC), Nigeria, as well as the support of Standards Organisation of Nigeria (SON), Nigeria, are both appreciated. The research reported in this paper is part of the Project 51922064 supported by the National Natural Science Foundation of China (NSFC). The article processing charges (APC) for this article were funded by author 1—C.V.A., with support from MDPI's JMSE.

Institutional Review Board Statement: Not applicable.

Informed Consent Statement: Not applicable.

Data Availability Statement: The data supporting the reported results cannot be shared at this time, as it has been used in producing more publications on this research.

Acknowledgments: The authors acknowledge the technical support of Lancaster University Engineering Department and Library staff, especially during the COVID-19 pandemic. The provision of the Simscale Platform, the permissions granted by Simscale to use their open-source online platform, and the technical support of the Simscale support team are well acknowledged and appreciated. We also acknowledge Jonathan Petit of Trelleborg, Oil & Marine Department, for the permission to use Trelleborg's marine hose image in Figure 1. We are very grateful to the anonymous reviewers for their feedback on this submission and also grateful to the journal editors for the support in improving the quality of this manuscript.

Conflicts of Interest: The authors declare no conflict of interest. The funders had no role in the design of the study; in the collection, analyses, or interpretation of data; in the writing of the manuscript; or in the decision to publish the results.

References

1. Chesterton, C. A Global and Local Analysis of Offshore Composite Material Reeling Pipeline Hose, with FPSO Mounted Reel Drum. Ph.D. Thesis, Lancaster University, Lancaster, UK, 2020.
2. Amaechi, C.V. Novel Design, Hydrodynamics and Mechanics of Marine Hoses in Oil/Gas Applications. Ph.D. Thesis, Lancaster University, Lancaster, UK, 2022.
3. Odijie, A.C. Design of Paired Column Semisubmersible Hull. Ph.D. Thesis, Lancaster University, Lancaster, UK, 2016. Available online: https://eprints.lancs.ac.uk/id/eprint/86961/1/2016AgbomeriePhD.pdf (accessed on 14 June 2021).
4. Odijie, A.C.; Wang, F.; Ye, J. A review of floating semisubmersible hull systems: Column stabilized unit. *Ocean Eng.* **2017**, *144*, 191–202. [CrossRef]
5. Amaechi, C.V.; Wang, F.; Ye, J. Investigation on Hydrodynamic Characteristics, Wave–Current Interaction and Sensitivity Analysis of Submarine Hoses Attached to a CALM Buoy. *J. Mar. Sci. Eng.* **2022**, *10*, 120. [CrossRef]
6. Amaechi, C.V.; Wang, F.; Ja'e, I.A.; Aboshio, A.; Odijie, A.C.; Ye, J. A literature review on the technologies of bonded hoses for marine applications. *Ships Offshore Struct.* **2022**. [CrossRef]
7. Ochoa, O.; Salama, M. Offshore composites: Transition barriers to an enabling technology. *Compos. Sci. Technol.* **2005**, *65*, 2588–2596. [CrossRef]
8. Amaechi, C.V.; Ye, J. A numerical modeling approach to composite risers for deep waters. In *Structural and Computational Mechanics Book Series, Proceedings of the ICCS20 20th International Conference on Composite Structures, Paris, France, 4–7 September 2017*; Ferreira, A.J.M., Larbi, W., Deu, J.-F., Tornabene, F., Fantuzzi, N., Eds.; Societa Editrice Esculapio: Bologna, Italy, 2017; pp. 262–263.
9. Amaechi, C.V.; Gillett, N.; Odijie, A.C.; Hou, X.; Ye, J. Composite risers for deep waters using a numerical modelling approach. *Compos. Struct.* **2019**, *210*, 486–499. [CrossRef]
10. Amaechi, C.V.; Ye, J. Local tailored design of deep water composite risers subjected to burst, collapse and tension loads. *Ocean Eng.* **2021**, in press. [CrossRef]
11. Amaechi, C.V.; Gillett, N.; Odijie, A.C.; Wang, F.; Hou, X.; Ye, J. Local and global design of composite risers on truss SPAR platform in deep waters. In Proceedings of the 5th International Conference on Mechanics of Composites, Lisbon, Portugal, 1–4 July 2019; pp. 1–3. Available online: https://eprints.lancs.ac.uk/id/eprint/136431/4/Local_and_Global_analysis_of_Composite_Risers_MechComp2019_Conference_Victor.pdf (accessed on 23 November 2021).
12. Chibueze, N.O.; Ossia, C.V.; Okoli, J.U. On the fatigue of steel catenary risers. *Stroj. Vestn. J. Mech. Eng.* **2016**, *62*, 751–756. [CrossRef]
13. Ezeonwumelu, T.C.; Ossia, C.V.; Douglas, I.E. Fatigue damage of vertical rigid risers due to in-line vortex induced vibration in Nigeria shallow waters. *Am. J. Mech. Eng.* **2017**, *5*, 33–40. [CrossRef]
14. Akpan, V.; Ossia, C.V.; Fayemi, F. On the study of wellhead fatigue due to vortex induced vibration in the Gulf of Guinea. *J. Mech. Eng. Autom.* **2017**, *7*, 8–15. [CrossRef]
15. Udeze, K.U.; Ossia, C.V. Vortex induced vibration of subsea umbilicals: A case study of deep offshore Nigeria. *Univers. J. Mech. Eng.* **2017**, *5*, 35–46. [CrossRef]
16. Amaechi, C.V.; Wang, F.; Ye, J. Mathematical modelling of marine bonded hoses for single point mooring (SPM) systems, with catenary anchor leg mooring (CALM) buoy application—A review. *J. Mar. Sci. Eng.* **2021**, *9*, 1179. [CrossRef]
17. Amaechi, C.V.; Chesterton, C.; Butler, H.O.; Wang, F.; Ye, J. Review on the design and mechanics of bonded marine hoses for catenary anchor leg mooring (CALM) buoys. *Ocean Eng.* **2021**, *242*, 110062. [CrossRef]
18. Amaechi, C.V.; Chesterton, C.; Butler, H.O.; Wang, F.; Ye, J. An overview on bonded marine hoses for sustainable fluid transfer and (un)loading operations via floating offshore structures (FOS). *J. Mar. Sci. Eng.* **2021**, *9*, 1236. [CrossRef]
19. Amaechi, C.V.; Ye, J.; Hou, X.; Wang, F.-C. Sensitivity Studies on offshore submarine hoses on CALM buoy with comparisons for Chinese-lantern and lazy-S configuration. In Proceedings of the 38th International Conference on Ocean, Offshore and Arctic Engineering, Glasgow, UK, 9–14 June 2019.

20. Pham, D.-C.; Sridhar, N.; Qian, X.; Sobey, A.; Achintha, M.; Shenoi, A. A review on design, manufacture and mechanics of composite risers. *Ocean Eng.* **2016**, *112*, 82–96. [CrossRef]
21. Toh, W.; Bin Tan, L.; Jaiman, R.K.; Tay, T.E.; Tan, V.B.C. A comprehensive study on composite risers: Material solution, local end fitting design and local design. *Mar. Struct.* **2018**, *61*, 155–169. [CrossRef]
22. Lassen, T.; Eide, A.L.; Meling, T.S. Ultimate strength and fatigue durability of steel reinforced rubber loading hoses. In Proceedings of the ASME 2010 29th International Conference on Ocean, Offshore and Arctic Engineering, Shanghai, China, 6–11 June 2010; Volume 5, pp. 277–286. [CrossRef]
23. Tonatto, M.L.; Tita, V.; Forte, M.M.; Amico, S.C. Multi-scale analyses of a floating marine hose with hybrid polyaramid/polyamide reinforcement cords. *Mar. Struct.* **2018**, *60*, 279–292. [CrossRef]
24. Tonatto, M.L.; Roese, P.B.; Tita, V.; Forte, M.M.; Amico, S.C. Chapter 14: Offloading marine hoses: Computational and experimental analyses. In *Marine Composites*; Pemberton, R., Summerscales, J., Graham-Jones, J., Eds.; Woodhead Publishing Series in Composites Science and Engineering; Woodhead Publishing: Sawston, UK, 2019; pp. 89–416. [CrossRef]
25. Donnell, L.H. *Stability of Thin-Walled Tubes Under Torsion*; Technical Report for NASA; NASA: Washington, DC, USA, 1933; p. 479. Available online: https://ntrs.nasa.gov/citations/19930091553 (accessed on 23 November 2021).
26. Guz, I.A.; Menshykova, M.; Paik, J.K. Thick-walled composite tubes for offshore applications: An example of stress and failure analysis for filament-wound multi-layered pipes. *Ships Offshore Struct.* **2017**, *12*, 304–322. [CrossRef]
27. Zheng, J.; Liu, P. Elasto-plastic stress analysis and burst strength evaluation of Al-carbon fiber/epoxy composite cylindrical laminates. *Comput. Mater. Sci.* **2008**, *42*, 453–461. [CrossRef]
28. Amaechi, C.V.; Wang, F.; Hou, X.; Ye, J. Strength of submarine hoses in Chinese-lantern configuration from hydrodynamic loads on CALM buoy. *Ocean Eng.* **2018**, *171*, 429–442. [CrossRef]
29. Amaechi, C.V.; Wang, F.; Ye, J. Numerical Assessment on the Dynamic Behaviour of Submarine Hoses Attached to CALM Buoy Configured as Lazy-S under Water Waves. *J. Mar. Sci. Eng.* **2021**, *9*, 1130. [CrossRef]
30. Amaechi, C.V.; Wang, F.; Ye, J. Understanding the fluid-structure interaction from wave diffraction forces on CALM buoys: Numerical and analytical solutions. *Ships Offshore Struct.* **2021**, in press. [CrossRef]
31. Amaechi, C.V.; Wang, F.; Ye, J. Numerical studies on CALM buoy motion responses and the effect of buoy geometry cum skirt dimensions with its hydrodynamic waves-current interactions. *Ocean Eng.* **2022**, *244*, 110378. [CrossRef]
32. Yokohama. *Seaflex Yokohama Offshore Loading & Discharge Hose*; The Yokohama Rubber Co. Ltd.: Hiratsuka City, Japan, 2016. Available online: https://www.y-yokohama.com/global/product/mb/pdf/resource/seaflex.pdf (accessed on 17 May 2021).
33. Trelleborg. *Oil & Gas Solutions: Oil & Gas Hoses for Enhanced Fluid Transfer Solutions*; Trelleborg: Clemont-Ferrand, France, 2018; Volume 1, pp. 1–30.
34. Continental. *Continental Marine Hose Brochure*; Dunlop Oil & Marine: Grimsby, UK, 2020. Available online: https://aosoffshore.com/wp-content/uploads/2020/02/ContiTech_Marine-Brochure.pdf (accessed on 17 February 2021).
35. EMSTEC. *EMSTEC Loading & Discharge Hoses for Offshore Moorings*; EMSTEC: Rosengarten, Germany, 2016. Available online: https://denialink.eu/pdf/emstec.pdf (accessed on 29 September 2021).
36. OIL. *Offloading Hoses*; Offspring International Limited: Dudley, UK, 2020. Available online: https://www.offspringinternational.com/wp-content/uploads/2020/06/OIL-Offloading-Hoses-Brochure-2020-W.pdf (accessed on 19 August 2021).
37. Wang, C.; Shankar, K.; Morozov, E.V. Tailored design of top-tensioned composite risers for deep-water applications using three different approaches. *Adv. Mech. Eng.* **2017**, *9*, 1–18. [CrossRef]
38. Wang, C.; Ge, S.; Sun, M.; Jia, Z.; Han, B. Comparative study of vortex-induced vibration of FRP composite risers with large length to diameter ratio under different environmental situations. *Appl. Sci.* **2019**, *9*, 517. [CrossRef]
39. Wang, C.; Sun, M.; Shankar, K.; Xing, S.; Zhang, L. CFD simulation of vortex induced vibration for FRP composite riser with different modeling methods. *Appl. Sci.* **2018**, *8*, 684. [CrossRef]
40. Van Onna, M.; Lyon, J. Installation of World's 1st Subsesa Thermoplastic Composite Pipe Jumper on Alder. Available online: https://www.subseauk.com/documents/presentations/martin%20van%20onna%20-%20fields%20of%20the%20future%20-%20airborne.pdf (accessed on 23 November 2021).
41. Van Onna, M.; Gioccobi, S.; de Boer, H. Evaluation of the first deployment of a composite downline in deepwater Brazil. In Proceedings of the Rio Oil & Gas Expo and Conference, Rio De Janeiro, Brazil, 15–18 September 2014; pp. 1–9.
42. Roberts, D.; Hatton, S.A. Development and qualification of end fittings for composite riser pipe. In Proceedings of the Offshore Technology Conference, Houston, TX, USA, 6–9 May 2013. [CrossRef]
43. Van Onna, M.; O'Brien, P. A new thermoplastic composite riser for deepwater application. In *Subsea UK Conference*; Subsea UK News: Aberdeen, UK, 2011; pp. 1–23. Available online: https://www.subseauk.com/documents/martinvanonnasubsea2011presentation.pdf (accessed on 23 November 2021).
44. Smits, A.; Neto, T.B.; de Boer, H. Thermoplastic composite riser development for ultradeep water. In Proceedings of the Offshore Technology Conference, Houston, TX, USA, 30 April–3 May 2018; pp. 1–9. [CrossRef]
45. MagmaGlobal. Ocyan–Magma CompRisers. Available online: https://www.magmaglobal.com/risers/ocyan-compriser/ (accessed on 23 May 2021).

46. Yang, C.; Kang, Z. Assessment of Fatigue Damage Initiation in FPSO's Oil Offloading Line in West Africa. In Proceedings of the 28th International Ocean and Polar Engineering Conference, Sapporo, Japan, 10–15 June 2018. Available online: https://onepetro.org/ISOPEIOPEC/proceedings-abstract/ISOPE18/All-ISOPE18/ISOPE-I-18-109/20158 (accessed on 23 November 2021).
47. Amaechi, C.V.; Adefuye, E.F.; Oyetunji, A.K.; Ja'E, I.A.; Adelusi, I.; Odijie, A.C.; Wang, F. Numerical study on plastic strain distributions and mechanical behaviour of a tube under bending. *Inventions* **2022**, *7*, 9. [CrossRef]
48. Tonatto, M.L.; Tita, V.; Araujo, R.T.; Forte, M.M.; Amico, S.C. Parametric analysis of an offloading hose under internal pressure via computational modelling. *Mar. Struct.* **2017**, *51*, 174–187. [CrossRef]
49. Gao, P.; Gao, Q.; An, C.; Zeng, J. Analytical modeling for offshore composite rubber hose with spiral stiffeners under internal pressure. *J. Reinf. Plast. Compos.* **2020**, *40*, 352–364. [CrossRef]
50. Tonatto, M.L.; Forte, M.M.; Tita, V.; Amico, S.C. Progressive damage modeling of spiral and ring composite structures for offloading hoses. *Mater. Des.* **2016**, *108*, 374–382. [CrossRef]
51. Tonatto, M.L.; Forte, M.M.C.; Amico, S.C. Compressive-tensile fatigue behavior of cords/rubber composites. *Polym. Test.* **2017**, *61*, 185–190. [CrossRef]
52. Yu, K.; Morozova, E.V.; Ashrafa, M.A.; Shankar, K. A review of the design and analysis of reinforced thermoplastic pipes for offshore applications. *J. Reinf. Plast. Compos.* **2017**, *36*, 1514–1530. [CrossRef]
53. Yu, K.; Morozova, E.V.; Ashrafa, M.A.; Shankar, K. Numerical analysis of the mechanical behaviour of reinforced thermoplastic pipes under combined external pressure and bending. *Compos. Struct.* **2015**, *131*, 453–461. [CrossRef]
54. Gu, F.; Huang, C.-K.; Zhou, J.; Li, L.-P. Mechanical response of steel wire wound reinforced rubber flexible pipe under internal pressure. *J. Shanghai Jiaot. Univ. Sci.* **2009**, *14*, 747–756. [CrossRef]
55. Xu, Y.; Fang, P.; Bai, Y. Mechanical behavior of metallic strip flexible pipes during reeling operation. *Mar. Struct.* **2021**, *77*, 102942. [CrossRef]
56. Hirdaris, S.; Bai, W.; Dessi, D.; Ergin, A.; Gu, X.; Hermundstad, O.; Huijsmans, R.; Iijima, K.; Nielsen, U.; Parunov, J.; et al. Loads for use in the design of ships and offshore structures. *Ocean. Eng.* **2014**, *78*, 131–174. [CrossRef]
57. O'Donoghue, T. The Dynamic Behaviour of a Surface Hose Attached to a CALM Buoy. Ph.D. Thesis, Heriot-Watt University, Edinburgh, UK, 1987. Available online: https://www.ros.hw.ac.uk/handle/10399/1045?show=full (accessed on 17 May 2021).
58. O'Donoghue, T.; Halliwell, A.R. Vertical bending moments and axial forces in a floating marine hose-string. *Eng. Struct.* **1990**, *12*, 124–133. [CrossRef]
59. O'Donoghue, T.; Halliwell, A.R. Floating hose-strings attached to a calm buoy. In Proceedings of the Offshore Technology Conference, Houston, TX, USA, 2–5 May 1988. [CrossRef]
60. Focke, E.S. Reeling of Tight Fit Pipe. Ph.D. Thesis, Delft University of Technology, Delft, The Netherlands, 2007. Available online: http://resolver.tudelft.nl/uuid:21348ba3-bce9-4b01-98fd-f1a32fafaaa9 (accessed on 19 August 2021).
61. Nooij, S. Feasibility of IGW Technology in Offloading Hoses. Master's Thesis, Delft University of Technology, Delft, The Netherlands, 2006. Available online: http://resolver.tudelft.nl/uuid:4617e7a0-b5d8-4c86-94d5-8d2037b31769 (accessed on 19 August 2021).
62. Bai, Y.; Xu, F.; Cheng, P.; Badaruddin, M.F.; Ashri, M. Burst Capacity of Reinforced Thermoplastic Pipe (RTP) Under Internal Pressure. In Proceedings of the ASME 2011 30th International Conference on Ocean, Offshore and Arctic Engineering, Rotterdam, The Netherlands, 19–24 June 2011; Volume 4, pp. 281–288. [CrossRef]
63. Bai, Y.; Liu, T.; Cheng, P.; Yuan, S.; Yao, D.; Tang, G. Buckling stability of steel strip reinforced thermoplastic pipe subjected to external pressure. *Compos. Struct.* **2016**, *152*, 528–537. [CrossRef]
64. Zhou, Y.; Duan, M.; Ma, J.; Sun, G. Theoretical analysis of reinforcement layers in bonded flexible marine hose under internal pressure. *Eng. Struct.* **2018**, *168*, 384–398. [CrossRef]
65. Zheng, J.-Y.; Gao, Y.-J.; Li, X.; Lin, X.-F.; Lu, Y.-B.; Zhu, Y.-C. Investigation on short-term burst pressure of plastic pipes reinforced by cross helically wound steel wires. *J. Zhejiang Univ. Sci. A* **2008**, *9*, 640–647. [CrossRef]
66. Lipski, W. Mechanical Lined Pipe—Installation by Reel-Lay. p. 17. Available online: https://www.yumpu.com/en/document/read/26877695/mechanical-lined-pipe-installation-by-reel-lay-subsea-uk (accessed on 19 August 2021).
67. Muren, J.; Caveny, K.; Eriksen, M.; Viko, N.G.; MÜLler-Allers, J.; JØRgen, K.U. *Un-Bonded Flexible Risers–Recent Field Experience and Actions for Increased Robustness*; 0389-26583-U-0032, Revision 5.0; PSA: Asker, Norway, 2013; Volume 2, pp. 1–78. Available online: https://www.ptil.no/contentassets/c2a5bd00e8214411ad5c4966009d6ade/un-bonded-flexible-risers--recent-field-experience-and-actions--for-increased-robustness.pdf (accessed on 17 June 2021).
68. Løtveit, S.A.; Muren, J.; Nilsen-Aas, C. *Bonded Flexibles–State of the Art Bonded Flexible Pipes*; 26583U-1161480945-354, Revision 2.0, Approved on 17.12.2018; PSA: Asker, Norway, 2018; pp. 1–75. Available online: https://www.4subsea.com/wp-content/uploads/2019/01/PSA-Norway-State-of-the-art-Bonded-Flexible-Pipes-2018_4Subsea.pdf (accessed on 17 June 2021).
69. Edward, C.; Dev, A.K. Assessment of CALM buoys motion response and dominant OPB/IPB inducing parameters on fatigue failure of offshore mooring chains. In *Practical Design of Ships and Other Floating Structures, Proceedings of PRADS 2009 Conference*; Springer International Publishing: Berlin/Heidelberg, Germany, 2020; Volume 64, pp. 548–579. [CrossRef]
70. Jean, P.; Goessens, K.; L'hostis, D. Failure of chains by bending on deepwater mooring systems. In Proceedings of the Offshore Technology Conference, Houston, TX, USA, 2–5 May 2005. [CrossRef]
71. Shoup, G.J.; Mueller, R.A. Analysis of a calm buoy anchor chain system. In Proceedings of the Offshore Technology Conference, Houston, TX, USA, 7–9 May 1984. [CrossRef]

72. Xia, M.; Takayanagi, H.; Kemmochi, K. Analysis of multi-layered filament-wound composite pipes under internal pressure. *Compos. Struct.* **2001**, *53*, 483–491. [CrossRef]
73. Sun, C.T.; Li, S. Three-dimensional effective elastic constant for thick laminates. *J. Compos. Mater.* **1988**, *22*, 629–639. [CrossRef]
74. Ye, J.; Soldatos, K.P. Three-dimensional buckling analysis of laminated composite hollow cylinders and cylindrical panels. *Int. J. Solid Struct.* **1995**, *32*, 1949–1962. [CrossRef]
75. Bakaiyan, H.; Hosseini, H.; Ameri, E. Analysis of multi-layered filament-wound composite pipes under combined internal pressure and thermomechanical loading with thermal variations. *Compos. Struct.* **2009**, *88*, 532–541. [CrossRef]
76. Gao, Q.; Zhang, P.; Duan, M.; Yang, X.; Shi, W.; An, C.; Li, Z. Investigation on structural behavior of ring-stiffened composite offshore rubber hose under internal pressure. *Appl. Ocean. Res.* **2018**, *79*, 7–19. [CrossRef]
77. Nassiraei, H.; Rezadoost, P. Static capacity of tubular X-joints reinforced with fiber reinforced polymer subjected to compressive load. *Eng. Struct.* **2021**, *236*, 112041. [CrossRef]
78. Nassiraei, H.; Rezadoost, P. Local joint flexibility of tubular T/Y-joints retrofitted with GFRP under in-plane bending moment. *Mar. Struct.* **2021**, *77*, 102936. [CrossRef]
79. Gonzalez, G.M.; Sousa, J.R.M.; Sagrilo, L.V.S. A study on the axial behavior of bonded flexible marine hoses. *Mar. Syst. Ocean Technol.* **2016**, *11*, 31–43. [CrossRef]
80. Fergestad, D.; Løtveit, S.A. *Handbook on Design and Operation of Flexible Pipes*; SINTEF: Trondheim, Norway, 2014. Available online: https://core.ac.uk/download/pdf/52134083.pdf (accessed on 17 November 2021).
81. Lassen, T.; Lem, A.I.; Imingen, G. Load response and finite element modelling of bonded loading hoses. In Proceedings of the ASME 2014 33rd International Conference on Ocean, Offshore and Arctic Engineering, San Francisco, CA, USA, 8–13 June 2014; Volume 6A. [CrossRef]
82. Tonatto, M.L.; Tita, V.; Amico, S.C. Composite spirals and rings under flexural loading: Experimental and numerical analysis. *J. Compos. Mater.* **2020**, *54*, 2697–2705. [CrossRef]
83. ANSYS. *ANSYS Modeling and Meshing Guide. Release 9.0*; ANSYS Inc.: Canonsburg, PA, USA, 2004. Available online: http://dl.mycivil.ir/reza/Ansys%20Modeling%20And%20Meshing%20Guide.pdf (accessed on 27 August 2021).
84. ANSYS. *ANSYS Meshing User's Guide, Release 15.0*; ANSYS Inc.: Canonsburg, PA, USA, 2013. Available online: https://www.academia.edu/27974461/ANSYS_Meshing_Users_Guide (accessed on 19 August 2021).
85. Simscale Documentation. Available online: https://www.simscale.com/docs/ (accessed on 19 August 2021).
86. Rabelo, A.S. Estudo Do Comportamento De Mangueiras Termoplásticas De Umbilicais Submarinos Submetidas A Carregamentos Mecânicos. Master's Thesis, Universidade Federal do Rio de Janeiro (UFRJ) & COPPE, Rio de Janeiro, Brasil, 2013. Available online: https://w1files.solucaoatrio.net.br/atrio/ufrj-peno_upl//THESIS/6000252/2013_mestrando_alexandre_soares_rabelo_20200405214916875.pdf (accessed on 27 August 2021).
87. Muren, J. *PSA—Norway Flexible Pipe: Failure Modes, Inspection, Testing and Monitoring*; PSA Norway: Asker, Norway, 2007. Available online: https://www.ptil.no/contentassets/a4c8365164094826a24499ef9f22742b/p5996rpt01rev02cseaflex_janmuren.pdf (accessed on 29 July 2021).
88. Drumond, G.P.; Pasqualino, I.; Pinheiro, B.; Estefen, S. Pipelines, risers and umbilicals failures: A literature review. *Ocean Eng.* **2018**, *148*, 412–425. [CrossRef]
89. Simonsen, A. Inspection and Monitoring Techniques for Un-Bonded Flexible Risers and Pipelines. Master's Thesis, University of Stavanger, Stavanger, Norway, 2014. Available online: http://hdl.handle.net/11250/219671 (accessed on 27 August 2021).
90. Hirdaris, S.E.; Lees, A.W. A conforming unified finite element formulation for the vibration of thick beams and frames. *Int. J. Numer. Methods Eng.* **2004**, *62*, 579–599. [CrossRef]
91. Timoshenko, S.P. LXVI. On the correction of shear of the differential equation for transverse vibrations of prismatic bars. *Lond. Edinb. Dublin Philos. Mag. J. Sci.* **1921**, *41*, 744–746. [CrossRef]
92. Timoshenko, S.P. X. On the transverse vibrations of bars of uniform cross-section. *Lond. Edinb. Dublin Philos. Mag. J. Sci.* **1921**, *43*, 125–131. [CrossRef]
93. Timoshenko, S.; Woinowsky-krieger, S. *Theory of Plates and Shells*, 2nd ed.; McGraw-Hill: New York, NY, USA, 1959; pp. 1–566.
94. API. *API 17K. Specification for Bonded Flexible Pipe*, 3rd ed.; American Petroleum Institute (API): Houston, TX, USA, 2017.
95. ISO. *ISO 13628-10. Petroleum and Natural Gas Industries–Design and Operation of Subsea Production Systems–Part 10: Specification for Bonded Flexible Pipe*; International Organization for Standardization (ISO): Geneva, Switzerland, 2005.
96. DNVGL. *DNVGL-OS-E403. Offshore Loading Buoys*; Det Norske Veritas & Germanischer Lloyd: Oslo, Norway, 2015. Available online: https://rules.dnv.com/docs/pdf/DNV/os/2015-07/DNVGL-OS-E403.pdf (accessed on 29 July 2021).
97. ABS. *Rules For Building And Classing–Single Point Moorings*; American Bureau of Shipping (ABS): Houston, TX, USA, 2014. Available online: https://ww2.eagle.org/content/dam/eagle/rules-and-guides/current/offshore/8_rules-forbuildingandclassingsinglepointmoorings_2021/spm-rules-jan21.pdf (accessed on 29 July 2021).
98. OCIMF. *Single Point Mooring Maintenace and Operations Guide (SMOG)*; Witherby & Co. Ltd: London, UK, 1995.
99. OCIMF. *Guide to Manufacturing and Purchasing Hoses for Offshore Moorings (GMPHOM)*; Witherby Seamanship International Ltd.: Livingstone, UK, 2009.
100. Wahl, A.M. *Mechanical Springs*, 1st ed.; Penton Publishing Company: Cleveland, OH, USA, 1944.